Biogeosciences, 7, 1833–1859, 2010
www.biogeosciences.net/7/1833/2010/
doi:10.5194/bg-7-1833-2010

Biogeosciences

Optimisation of photosynthetic carbon gain and within-canopy gradients of associated foliar traits for Amazon forest trees

J. Lloyd[1], S. Patiño[2], R. Q. Paiva[3,*], G. B. Nardoto[4], C. A. Quesada[1,3,5], A. J. B. Santos[3,5,†], T. R. Baker[1], W. A. Brand[6], I. Hilke[6], H. Gielmann[6], M. Raessler[6], F. J. Luizão[3], L. A. Martinelli[4], and L. M. Mercado[7]

[1]Earth and Biosphere Institute, School of Geography, University of Leeds, LS2 9JT, UK
[2]Grupo de Ecología de Ecosistemas Terrestres Tropicales, Universidad Nacional de Colombia, Sede Amazonia, Instituto Amazónico de Investigaciones-Imani, km. 2, vía Tarapacá, Leticia, Amazonas, Colombia
[3]Institito National de Pesquisas Amazônicas, Manaus, Brazil
[4]Centro de Energia Nuclear na Agricultura, Av. Centenário 303, 13416-000, Piracicaba-SP, Brazil
[5]Departamento de Ecologia, Universidade de Brasília, DF, Brazil
[6]Max-Planck-Institut für Biogeochemie, Postfach 100164, 07701, Jena, Germany
[7]Centre for Ecology and Hydrology, Wallingford, UK
[*]now at: Secretária Municipal de Desenvolvimento e Meio Ammbiente ma Prefeturia Municipal de Maués, Maués, Brazil
[†]Alexandre Santos died in the Amazon plane crash of 29 September 2006

Received: 18 December 2008 – Published in Biogeosciences Discuss.: 5 May 2009
Revised: 24 March 2010 – Accepted: 15 April 2010 – Published: 4 June 2010

Abstract. Vertical profiles in leaf mass per unit leaf area (M_A), foliar ^{13}C composition ($\delta^{13}C$), nitrogen (N), phosphorus (P), carbon (C) and major cation concentrations were estimated for 204 rain forest trees growing in 57 sites across the Amazon Basin. Data was analysed using a multilevel modelling approach, allowing a separation of gradients within individual tree canopies (within-tree gradients) as opposed to stand level gradients occurring because of systematic differences occurring between different trees of different heights (between-tree gradients). Significant positive within-tree gradients (i.e. increasing values with increasing sampling height) were observed for M_A and $[C]_{DW}$ (the subscript denoting on a dry weight basis) with negative within-tree gradients observed for $\delta^{13}C$, $[Mg]_{DW}$ and $[K]_{DW}$. No significant within-tree gradients were observed for $[N]_{DW}$, $[P]_{DW}$ or $[Ca]_{DW}$. The magnitudes of between-tree gradients were not significantly different to the within-tree gradients for M_A, $\delta^{13}C$, $[C]_{DW}$, $[K]_{DW}$, $[N]_{DW}$, $[P]_{DW}$ and $[Ca]_{DW}$. But for $[Mg]_{DW}$, although there was no systematic difference observed between trees of different heights, strongly negative within-tree gradients were found to occur.

When expressed on a leaf area basis (denoted by the subscript "A"), significant positive gradients were observed for $[N]_A$, $[P]_A$ and $[K]_A$ both within and between trees, these being attributable to the positive intra- and between-tree gradients in M_A mentioned above. No systematic within-tree gradient was observed for either $[Ca]_A$ or $[Mg]_A$, but with a significant positive gradient observed for $[Mg]_A$ between trees (i.e. with taller trees tending to have a higher Mg per unit leaf area).

Significant differences in within-tree gradients between individuals were observed only for M_A, $\delta^{13}C$ and $[P]_A$. This was best associated with the overall average $[P]_A$ for each tree, this also being considered to be a surrogate for a tree's average leaf area based photosynthetic capacity, A_{max}. A new model is presented which is in agreement with the above observations. The model predicts that trees characterised by a low upper canopy A_{max} should have shallow, or even non-existent, within-canopy gradients in A_{max}, with optimal intra-canopy gradients becoming sharper as a tree's

Correspondence to: J. Lloyd
(j.lloyd@leeds.ac.uk)

upper canopy A_{max} increases. Nevertheless, in all cases it is predicted that the optimal within-canopy gradient in A_{max} should be substantially less than for photon irradiance. Although this is also shown to be consistent with numerous observations as illustrated by a literature survey of gradients in photosynthetic capacity for broadleaf trees, it is also in contrast to previously held notions of optimality. A new equation relating gradients in photosynthetic capacity within broadleaf tree canopies to the photosynthetic capacity of their upper canopy leaves is presented.

1 Introduction

It has long been observed that the light saturated photosynthetic rates of leaves located low in plant canopies can be much less than leaves receiving much more irradiance (Q) higher up (Jarvis et al., 1976), and this has been typically attributed to gradients in foliar nitrogen contents on a leaf area basis (Field, 1983). Nitrogen is a critical component of the photosynthetic apparatus (Evans, 1989) and it has been shown that the theoretically optimal distribution of nitrogen concentration which maximizes canopy photosynthesis is that where the foliar nitrogen concentration gradient (leaf area basis) closely follows the distribution of Q, thus approaching zero when Q also does (Field, 1983; Chen et al., 1993). Nevertheless, one regular observation in tree canopies is that vertical gradients in photosynthetic capacity are much less than that associated with the optimal distribution maximising individual plant carbon gain (e.g. Hollinger, 1996; Kull and Niinemets, 1998; Meir et al., 2002; Wright et al., 2006).

Understanding and quantifying within-canopy gradients in photosynthetically important nutrients and associated changes in plant physiological properties is also important for simulating rates of canopy photosynthesis and the associated light response (Lloyd et al., 1995; Haxeltine and Prentice, 1996; de Pury and Farquhar, 1997; Mercado et al., 2009) as well as for simulations of canopy leaf areas (themselves affecting predicted rates of photosynthetic carbon gain) in dynamic vegetation models (Sitch et al., 2003; Woodward and Loomis, 2004). Within tropical forest canopies, this variation may be expected to be especially complicated due to the very high number of species present in any one forest with an associated high tree-to-tree variation (Fyllas et al., 2009), some of which can be related to asymptotic tree height (Lloyd et al., 1995; Thomas and Bazzaz, 1999; Rijkers et al., 2000), successional status (Popma et al., 1992; Reich et al., 1995) and/or shade tolerance (Turner, 2001). Mean vertical variations in nutrient concentrations and associated physiological characteristics within tropical forests may thus be as much due to tree-to-tree variations correlated with actual or greater osmotic potentials tree height as with variations within individual trees themselves.

Nitrogen need not, of course, always be the primary limiting nutrient for photosynthesis in higher plants (Field and Mooney, 1986). This may be especially the case for tropical forest trees whose photosynthetic rates may be more closely correlated with foliar phosphorus content (Cromer et al., 1993; Raaimakers et al., 1995; Reich et al., 1995; Lovelock et al., 1997; Domingues et al., 2010).

Associated with within-canopy gradients in photosynthetic capacity may also be gradients in foliar $\delta^{13}C$ which, rather than reflecting a substantial recycling of ^{13}C depleted carbon dioxide lower down plant canopies, probably reflects genuine vertical gradients in physiological processes for tropical forests (Lloyd et al., 1996). This could be attributable to upper canopy leaves being exposed to more severe water deficits during the day (Niinemets et al., 2004), though for conifers at least, it is also associated with variations in foliar nitrogen concentrations (leaf area basis), and by implication variations in photosynthetic capacity (Duursma and Marshall, 2006).

Although not yet studied in any great detail to date, gradients in foliar cations within plant canopies also occur. For example, Grubb and Edwards (1982) found magnesium concentrations (dry weight basis) to decrease with height for a New Guinea montane rain forest, attributing this to the central role of Mg within chlorophyll complex and the tendency for shaded leaves to have higher chlorophyll concentrations (again, expressed on a dry weight basis) than more exposed leaves higher up (Björkman et al., 1981). Gradients in other physiologically important cations might also be anticipated. For example, potassium has a critical role, not only in stomatal function, but also as an important foliar omsoticum (Leigh and Wyn-Jones, 1984), potentially being required in higher concentrations for leaves towards the top of the canopy where gas exchange rates would be expected to be higher (Carswell et al., 2000) and with the leaves there also tending to have greater osmotic potentials (Oberbauer et al., 1987).

We here analyse vertical variations in leaf properties for 204 trees sampled at a range of locations across Amazonia, attempting to quantify variations in nitrogen, phosphorus, major cations (Ca, Mg and K), carbon stable isotope composition and M_A with height. As well as analysing this observational data, we also present a new model which shows that the true "optimal" gradient in plant canopies does not necessarily mimic the gradient in Q. This model, described immediately below, is predicated on the observation that foliar leaf nutrient concentrations are to a large degree genetically constrained (Fyllas et al., 2009) and thus for any given species there is a practical limit for the maximum nutrient concentration possible. Once this is taken into account, it emerges that trees with a low overall photosynthetic potential should have a shallow (or even zero) decline in photosynthetic capacity with canopy depth, with higher photosynthetic capacity trees having sharper gradients for the optimisation of canopy photosynthesis. But with the predicted optimal gradients still

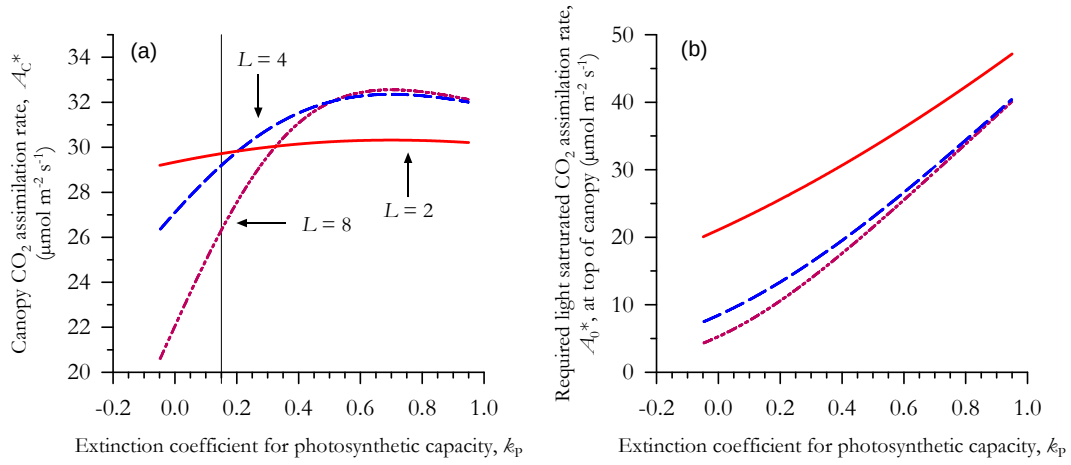

Fig. 1. Effect of variations in extinction coefficient for photosynthetic capacity, k_P at a range of different leaf area indices, L, for an overall canopy photosynthetic capacity (C_C) of 42 μmol m^{-2} s^{-1} (ground area basis) and at an incoming photon irradiance of 2000 μmol m^{-2} s^{-1} **(a)** Variations in canopy CO_2 assimilation rate (in the absence of any leaf respiration); **(b)** required CO_2 assimilation rate for the uppermost canopy leaves (A_0^*) in order to fulfill the requirements of Eq. (1).

substantially shallower than the within-canopy light profile. Data from a range of Amazon forest trees presented here suggests this to be the case, with these results also being confirmed through a global survey of vertical gradients of photosynthetic capacity within the canopies of broadleaf trees and forests.

2 Theoretical considerations

The model used to evaluate the optimal distribution of resources for species of a fixed maximum photosynthetic capacity is outlined in Appendix A. In short, it consists of the use of integral equations combining gradients in photosynthetically active radiation, Q, photosynthetic capacity, A_{max}, and leaf respiration, R, throughout plant canopies, also allowing for leaf respiration rates to be reduced at higher irradiances (Atkin et al., 2000). Gradients in Q and A_{max} are expressed in terms of exponential decay coefficients and are expressed as a function of canopy depth, this being defined for any point within the canopy (z) as the cumulative leaf area index measured downwards from the canopy top. That is to say, z=0 for the uppermost leaves of the canopy and z=L for the lowermost canopy leaves, with L being the canopy leaf area index.

2.1 Simulations with a canopy of fixed photosynthetic capacity

We first apply the model above to a rain forest canopy with L of either 2.0, 5.0 or 8.0, but in all cases having the same photosynthetic capacity, denoted here as C_C. To obtain a realistic estimate of the latter, we take representative observational values from data presented by Domingues et al. (2005) for a forest near Tapajós (Para State, Brazilian Amazon) *viz.* L=5.5, A_0^*=12.0 μmol m^{-2} s^{-1} (full sunlight) and with an extinction coefficient for photosynthetic capacity, k_P, of 0.15. Taking then a simple integral equation of the $A_{max(z)}$ term in Eq. (A2), we obtain

$$C_C = A_0^* e^{-k_P z}\Big|_{z=0}^{z=L} = \frac{A_0^*(1 - e^{-k_P L})}{k_P}, \quad (1)$$

where A_0^* is the maximum (light saturated) CO_2 assimilation rate at the top of the canopy, with the superscript "*" indicating that we are ignoring dark respiration. This yields C_C=42 μmol m^{-2} s^{-1} (ground area basis).

Now, keeping this canopy photosynthetic potential constant, the first question we ask in a series of investigative simulations is how should the canopy photosynthetic rate, A_C^*, vary across a range of potential k_P? And how is this variation in A_C^* with k_P influenced by L? To do this we use Eqs. (A4) and (A5) as detailed in Appendix A. For these simulations, we always use a value for the light extinction within the canopy of k_I=0.7 as reported for tropical forest (Wirth et al., 2001). Because C_C is held constant for all simulations, this requires that A_0^* varies as k_P changes. This is achieved via a rearrangement of Eq. (1) ; *viz.* A_0^*=$k_P C_C/(1-e^{-k_P L})$. Using the above procedure, we can thus estimate how A_C^* and A_0^* should vary with k_P for a given L and this is shown in Fig. 1. Figure 1a shows that, as expected from theory (Field, 1983), the maximum A_C^* is indeed always observed when $k_I = k_P = 0.7$. Also as expected, the higher the L, the greater the A_C^* at this optimum k_P. But as k_P declines (or increases) away from the optimum 0.7 value, the decline in A_C^* is much greater at higher L. So much so that at k_P=0.15 A_C^* actually declines with increasing L.

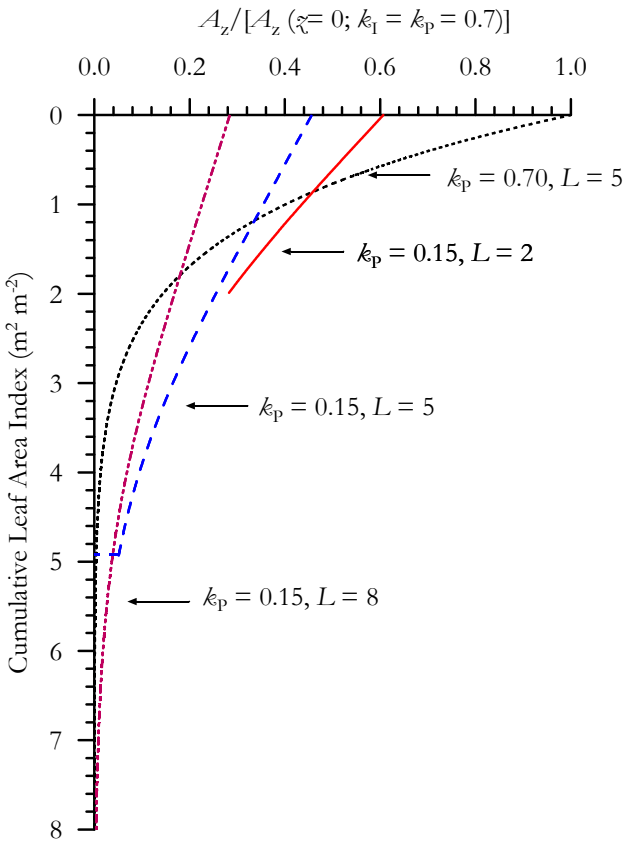

Fig. 2. Variations in the rate of photosynthesis at canopy depth z in the absence of dark respiration, A_z^*, normalised to that which would occur at the top of the canopy when the extinction coefficient for photosynthetic capacity, k_P, is equal to that for light, k_I which has in this case been set at 0.7. Values are shown for different combinations of k_P and leaf area index, L, at an incoming photon irradiance of 2000 µmol m^{-2} s^{-1}.

Figure 1b shows the changes in A_0^* required to satisfy Eq. (1) with C_C conserved. As k_P increases then so does A_0^*. Likewise, at any given k_P then if A_0^* is lower then a higher L is required. As has already been pointed out by Pons et al. (1990) for herbaceous species and Hollinger (1994) for the New Zealand tree *Nothofagus fusca*, Fig. 1b implies that there are certain combinations of A_0^*, k_P and C_C which may not be physiologically realistic. For example, most tropical tree species have maximum photosynthetic rates substantially less than 20 µmol m^{-2} s^{-1} (Turner, 2001, p. 97; Domingues et al., 2010). Thus an "optimum" k_P may not be possible in the case of Fig. 1b unless C_C were substantially lower (see Eq. 1). But this would then mean that A_C^* was also correspondingly reduced (again as shown in Sect. 2.3). This contradiction is the fundamental reason why "optima" k_P as implied by Fig. 1a are not, in fact, optimal at all. That is to say, if one accepts that there is a fundamental limit to the maximum photosynthetic rate possible for any given species (see also Sect. 6.1), then the sharp "optimum" k_P required for the gradient in photosynthetic capacity to match that of the light environment actually gives rise to a significantly lower canopy photosynthetic capacity were k_P to be substantially lower.

But why, despite higher canopy light interception, does A_C^* decline with increasing L at low k_P? This also turns out to be critical in Sect. 2.3 in determining what is the optimum L when C_C and A_0^* are taken as fixed. The answer can be seen from Fig. 2. Here, the required gradients in CO_2 assimilation rate in the absence of dark respiration (A^*) at depth z, A_z^*, are shown for various combinations of k_P and L with all values standardised to $A_0^* = 1.0$ when $k_I = k_P = 0.7$. As would be expected from Fig. 1b, when $k_P < 0.7$ then A_0^* is also less than this "optimal case" and as L increases the greater is the reduction in A_0^*. The vertical variation photosynthetic losses or gains associated with $k_P \neq 0.7$ can also easily be seen by comparing the A_z^* profiles for $k_P = 0.15$ with that for $k_P = 0.7$. This shows that, irrespective of L, and as would be expected, that A_z^* is lower towards the top of the canopy for lower k_P, but that this is to some degree compensated for by a greater A_z^* lower down. What can be seen from Fig. 2, however, is that the extent to which this higher A_z^* lower down in the canopy can compensate for lower A_z^* towards the top diminishes as L increases. As to why this occurs can be deduced from Fig. 1b. Because the high L/low k_P combination necessitates a low maximum photosynthetic capacity in the upper layers, much of the relatively high Q there cannot be utilised. On the other hand, a substantial proportion of the extra photosynthetic capacity lower down is more or less wasted as CO_2 assimilation rates at low Q are much less dependent on $A_{max(z)}$ (Fig. A1b). It is for this reason, as has also been noted by Hirose and Werger (1987), that the reduction in A_C^* as k_P deviates from its "optimum value" increases as L increases.

It is also worthwhile pointing out at this stage that the higher the value of A_0^* the greater the relative cost for any imbalances in the light versus photosynthetic capacity gradients at any given L. This is because any removal of photosynthetic capacity away from the top of the canopy results in a proportionally greater loss in A_C^* for high capacity as opposed to low capacity trees (see Fig. A1b).

2.2 What constitutes the optimal combination of L and k_P?

As argued above in Sect. 2.1, due to the high A_0^* required, what is often considered the "optimum" k_P may in fact not even be physiologically possible, especially when observation based values of C_C and L are employed. Indeed, it can even be argued that for such cases the "optimality" question may have been inappropriately posed. This is because, rather than asking what the optimum profile in photosynthetic capacity should be for given values of L and C_C, one should rather be inquiring as to, given the considerable genetic and environmental limitations on A_0^* that undoubtedly

occur (e.g. Wright et al., 2004; Fyllas et al., 2009); *What is the combination of L, C_C and k_P that serves to maximise the net carbon gain of the canopy for any given value of A_0^*?*

Such a simulation requires that one looks at timescales greater than hours or days, and so we drive the model using a dataset collected above the 87 km tower at Tapajós (Goulden et al., 2004) consisting of about 3.8 years of net (incoming less reflected) Q averaged over hourly times steps and running from 1 July 2000–11 March 2004. Using different symbols to identify the much longer timescales we are now working at, we write

$$N_R = G_C^* - R_C - I_C, \quad (2)$$

where N_R is the net carbon gain to the canopy provided by the foliage on an annual basis, after accounting for the investment of carbon as new leaves within the plant canopy (I_C) with R_C representing the annual respiratory losses by the canopy (estimated as detailed below) and G_C^* being the annual net carbon gain (Gross Primary Productivity) by the leaves in the absence of respiration in either the dark or the light. The latter is equivalent to A_C^*, calculated hourly, but summed over one year.

Noting also that elements such as nitrogen and phosphorus which are likely to be the key modulators of variations in $A_{max(z)}$ tend to stay constant on a dry weight basis with depth within the canopy and with variations on an area being due to variations in leaf mass per unit area (M_A), see Sect. 5.2 for Amazon trees and Sect. 6.1 for a general discussion, then it follows that the decline in C investment per unit leaf area with canopy depth should approximate that of the decline in photosynthetic capacity and it then follows that we can simply express I_C as

$$I_C = I_0 e^{-k_P z}\Big|_{z=0}^{z=L} = \frac{I_0(1 - e^{-k_P L})}{k_P}. \quad (3)$$

To estimate I_0 we assume an average leaf lifetime (τ) of one year and taking typical values of M_A and carbon content for upper canopy leaves at Tapajós (88.5 g m^{-2} and 491 mg g^{-1}, respectively) also accounting for construction respiration costs as in Masle et al. (1990) we obtain an estimate for I_0 of 4.5 mol C m^{-2} for an A_0^* of 12 µmol m^{-2} s^{-1}. Given that there is generally little correlation between photosynthetic capacity and M_A when the former is calculated on an area basis (Wright et al., 2004) we thus make I_0 independent of A_0 and as a simplification (also noting that it has no effect on the main conclusions of these simulations) we also make τ independent of A_{max} and I_0 (For a further discussion of the effects of these and other assumptions, see Sect. 6.3). A_C^* is calculated as in Eq. (A4) or Eq. (A5) and integrated annually to obtain G_C^*. Based on data of Domingues et al. (2005) night time respiration (R_n) is simply calculated as 0.08 C_C^* but with daytime respiration by the leaves within the canopy dependent upon the illumination received. The extent of any decline in leaf respiration rates during the day is specified to be through a paramaterisation of data presented by Atkin et al. (2000) as specified in Eq. (A7) or Eq. (A8) and as shown in Fig. A1b. The R_C values in Eq. (2) represent average annual sums.

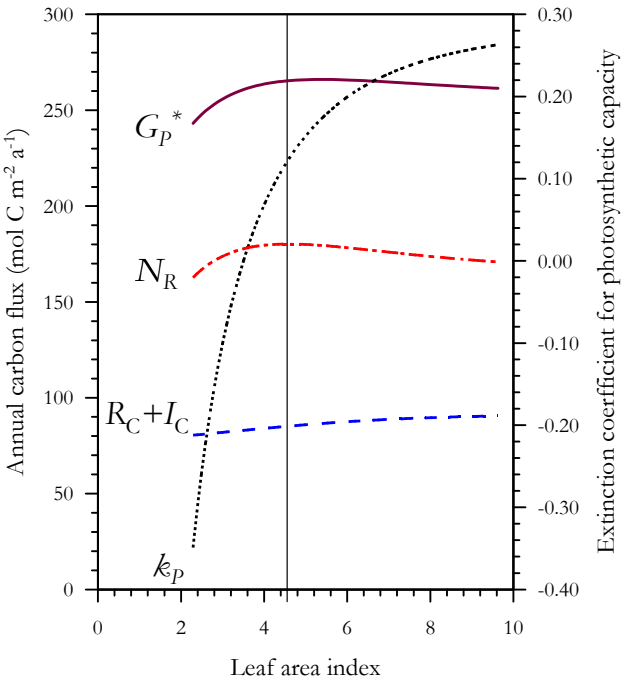

Fig. 3. Variations in the rate of Gross Primary production (in the absence of any leaf respiration in the light), G_P^*, the sum of leaf respiration (day and night) plus investment costs in leaf construction (R_C+I_C) and the difference between the two, the annual net carbon gain of the canopy, N_R as defined through Eq. (2) as a function of leaf area index, L. Associated variations in the extinction coefficient for photosynthetic capacity, k_P, are also shown, with the vertical line indicating the L associated with the maximisation of N_R.

Results from such a simulation are shown in Fig. 3 for our standard Tapajós conditions of A_0^*=12 µmol m^{-2} s^{-1} and C_C=42 µ mol m^{-2} s^{-1}. To create the curves, k_P has been increased in increments starting from a value of −0.35, with each output increment calculated to be sufficient to increase L by about 0.1. This has been achieved through L being calculated via a simple rearrangement of Eq. (1).

As k_P is increased, the gradient away from the top of the canopy must by definition become sharper. And associated with this an increase in L is required; this being necessary to "hold" the same C_C within a greater leaf area. Figure 3 shows that associated with this increase in k_P and L is first an increase in G_C^* associated with an increase in light interception. Nevertheless, as L increases above a value of ∼5.4 in this simulation, G_C^* begins to decline. This is because the aggravating effects of higher L on k_P/k_I imbalances as demonstrated in the previous Section (Fig. 2) outweigh the increasingly diminishing advantage of increased light interception.

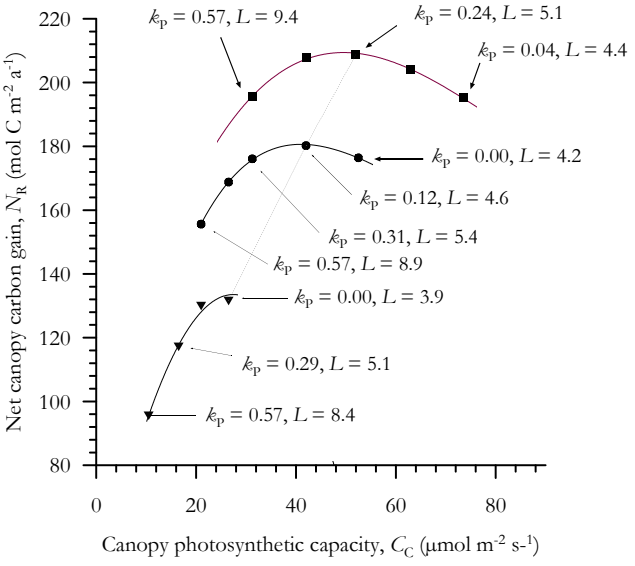

Fig. 4. Relationship between net canopy carbon gain (as defined by Eq. 2) and canopy photosynthetic capacity according to the model presented in Appendix A and Sect. 2. Curves shown are for different photosynthetic capacities, A_0^*, at the top of the canopy; ▼: A_0^*=6 μmol m^{-2} s^{-1}; ●: A_0^*=12 μmol m^{-2} s^{-1}; ■: A_0^*=18 μmol m^{-2} s^{-1}.

Although both I_C and night-time R_C do not change with the concurrent variations in k_P and L, daytime respiration increases. This is because associated with higher L are more and more leaves at very low light levels where the inhibition of daytime respiration is considerably reduced (Fig. A1a). Thus, the net carbon gain of the canopy, N_C, peaks at intermediate k_P and L: the optimum values from this simulation being 0.123 and 4.5, respectively. These values compare surprisingly favourably with what is actually observed for the Tapajós forest (k_P∼0.15) as discussed above with L=5.1±0.5 (Aragão et al., 2005). This may, however, be especially fortituous because, as is discussed in Appendix B, there are good reasons to think that both L and k_P should actually be a little higher than the simple estimates predicted here. We also note that an estimate for G_C^* of 262 mol C m^{-2} a^{-1} obtained from eddy covariance and other measurements at the Tapajós tower (Hutyra et al., 2007) is in remarkably good agreement with our model based estimate of G_C^* of 265 mol C m^{-2} a^{-1} at L=4.5.

It is also worth noting that although k_P<0.0 (i.e. photosynthetic capacities increasing with canopy depth) is both mathematically and physiologically possible, it is also at odds with one central tenant of the approach here (*viz*. that A_0^* is a maximum physiologically constrained value). Thus, although included in Fig. 2 for illustrative purposes, in the simulations which follow we limit our interpretations to cases where k_P≥0.0.

2.3 What constitutes the optimal combination of A_0^* and C_C?

In Sect. 2.2, we took our best estimate of the integrated canopy photosynthetic capacity for the Tapajós forest (A_0^*=12 μmol m^{-2} s^{-1} and C_C=42 μmol m^{-2} s^{-1}) and found that, although effects of variations in L and k_P on G_C^*, R_C and N_R were relatively modest, our model optimum N_R had associated with it values of G_C^*, L and k_P that were surprisingly close to those actually observed. But what happens with other combinations of A_0^* and C_C? To the extent that foliar nutrient concentrations are related to variations in leaf photosynthesis (Domingues et al., 2005, 2010; Mercado et al., 2009), A_0^* should reflect some combination of genetic and environmental influences (Fyllas et al., 2009). On the other hand, it might be reasonable to expect that the potential C_C for a given species would be more strongly influenced by edaphic conditions and/or climate than by genotype – this being mediated through variations in L and/or k_P.

To help answer this question, Fig. 4 shows the results of simulations where we have kept the model formulation and driving Q exactly as for Sect. 2.2, but investigating now how N_R varies for three different photosynthetic capacities at the top of the canopy, *viz* A_0^*=6 μmol m^{-2} s^{-1}, 12 μmol m^{-2} s^{-1} and 18 μmol m^{-2} s^{-1} and for a variety of C_C, the range of which examined depends on the A_0^* investigated. This selection has occurred because a high A_0^*/C_C ratio leads to unreasonably high L. Conversely a low A_0^*/C_C leads to k_P<0.0. In all cases, the symbol plotted reflects the value at the optimum N_R as determined from simulations such as shown in Fig. 3, Associated k_P and L are also shown for selected points.

This shows that, as might be anticipated, as C_C increases from the lowest values, then so does N_R. Associated with these increasing N_R are reductions in the optimal k_P. This allows a higher C_C to be more evenly distributed over a smaller L. Importantly, the lower L reduces overall respiratory losses. This is especially the case for high photosynthetic capacity leaves at the bottom of high C_C canopies. Yet, there is also a clear maximum for each A_0^*, beyond which N_R declines. This maximum occurs because the enhancement in G_C^* with higher C_C shows a shallower increment than the losses associated with R_C, including those at night. In short, above a certain point, little of the extra photosynthetic capacity can be put to good use. Though it still costs the tree in terms of respiratory carbon losses.

Not surprisingly, the C_C at which this point occurs increases with A_0^*; this being associated with a higher L and a higher k_P. For A_0^*=6 μmol m^{-2} s^{-1} the optimal prediction is no gradient in photosynthetic capacity at all. This is because such a tree should maximise its annual carbon gain by compressing as much photosynthetic potential into as small a leaf area as possible. As A_0^* increases the predicted "optimal" k_P also increases as a partitioning of resources, more

in-line with the light distribution, assume relatively more importance. This also being associated with a higher L. But in no case is the predicted k_P even close to that of the light extinction coefficient (k_I=0.7 in all simulations). Thus, our simulations here suggest that if physiological constraints on the maximum photosynthetic rate possible for upper-canopy leaves are taken into account along with the mutual dependencies of L and C_C and respiratory losses on k_P, then within canopy profiles of k_P should always be substantially less than k_I. This is because a low k_P gives a greater overall canopy photosynthetic capacity and thus a higher overall potential rate of carbon gain.

2.4 Model validation

For the remainder of this paper, we focus on gradients in key foliar properties such as leaf mass per unit area and foliar nitrogen and phosphorus concentrations within Amazon forest canopies. Taken together these three functional traits account for much of the variability in the photosynthetic rates of tropical trees (Domingues et al., 2010) thus providing good surrogates for variations in $A_{max(z)}$ (Sect. 5.3). Within the Discussion (Sect. 6.2), the extent to which the model accounts for variations observed for broadleaf tree k_P as a whole is also considered through a literature survey. Although variations in L are not explicitly considered in this data analysis, how model estimates of L and k_P may be modified by a consideration of evolutionarily stable versus instantaneous solutions (Anten, 2005) is considered in Appendix B.

3 Materials and methods

Of a total of 1508 trees sampled in 65 permanent plots in Brazil, Bolivia, Colombia, Ecuador, Peru and Venezuela between January 2002 and April 2005 for foliar nutrients and other properties (Fyllas et al., 2009; Patiño et al., 2009), 204 had also been sampled at three canopy heights for foliar nutrient composition, carbon and nitrogen isotope ratios and leaf mass per unit area (M_A). Locations, vegetation and basic soil and climatological characteristics of the sample material plots are given in Patiño et al. (2009) and Quesada et al. (2010).

3.1 Leaf sampling

Twelve to 40 trees per plot had been chosen at random for collection of upper canopy leaves. A professional tree climber usually climbed three to eight trees in different points of the plot. From each climbed tree, branches of 1 to 2 m length from the exposed crown of two to four nearby trees were also usually harvested. For randomly selected trees (generally three trees per plot) branches were additionally collected from the middle (sunny-shaded) and from the lower canopy (shaded) portion of the canopy. Sampling was achieved by severing a branch (usually ca. 4 cm in diameter) from the tree, this being subsequently allowed to fall to ground. From each branch a sub-sample was made, generally distal to the area of twig used by Patiño et al. (2009) for wood density analysis. One A4 sized plastic zip-bag of leaves of a range of possible different ages (but excluding obviously juvenile or senescencent leaves) was then filled and sealed, kept as cool and shaded as possible, and then transported to the laboratory or field station the same evening as the day of collection.

3.2 Tree and canopy height determinations

The heights of both the lowest branch and canopy of sample trees were determined using a clinometer (Model PM5/360 PC, Suunto, Turku, Finland) with "middle canopy" leaves assumed to have been at the average crown height; calculated as the arithmetic mean of the upper and lower crown dimensions.

3.3 Leaf mass per unit area (M_A)

Sub-samples of 10–20 leaves were taken for the leaves collected from each tree/measurement height combination and imaged using a locally purchased document scanner attached to a Laptop or PC. The scanned images were then saved as image files with leaf area and other associated characteristics of each image subsequently analysed using *Win Folia Basic 2001a* (Regent Instruments, Quebec, QC, Canada). Scanning was usually done on the evening of collection, but when for logistical reasons this was not possible, leaves were stored in a cool, dry, and shaded place in tightly sealed plastic bags for a maximum of two days to avoid desiccation and any associated reduction of the leaf area.

Once scanned, leaves were air dried in the field or when an oven was available they were dried at 70°C for about 24 h or with a microwave oven in 5 min steps until death was considered to have been achieved. Once transported to the analysis laboratory leaves were redried at 70 °C for about 24 h and their dry mass determined after being allowed to cool in a dessicator.

3.4 Sample preparation and analysis locations

Samples from Bolivia, Peru, Ecuador, Colombia and Venezuela were analysed in the Central Analytical and Stable Isotope Facilities at the Max-Planck Institute for Biogeochemistry (MPI-BGC) in Jena, Germany. Samples from the Brazilian sites were analysed for cations and phosphorus at the Instituto Nacional de Pesquisas da Amazônia (INPA) in Manaus and for carbon and nitrogen in the laboratory of the Empresa Brasileira de Pesquisa Agropecuária (EMBRAPA), also in Manaus. In both laboratories leaf sample not used for M_A determinations was dried as described above with a sub-sample of about 20 g DW then taken, for which the main

vein of all leaves was removed and the sub-sample subsequently ground. Sub-samples of ground material were also analysed for $^{13}C/^{12}C$ ratios (Sect. 3.7), the Brazilian analyses being undertaken at the Centro de Energia Nuclear na Agricultura (CENA) in Piracicaba.

3.5 Carbon and nitrogen determinations

In both laboratories, analyses for C and N were carried out using 15–30 mg of finely ground plant material using a "Vario EL" elemental analyser (Elementar Analysensysteme, Hanau, Germany). Inter-laboratory consistency was maintained via the regular use of the same CRM 101 spruce needle (Community Bureau of Reference, BCR, Brussels, Belgium) and SRM 1573a tomato leaf (National Institute of Standards of Technology, Gaithersburg, MD, USA) standards in both laboratories. Within the Manaus laboratory, laboratory consistency with Jena values was also checked from time to time by the comparison of ground rain forest tree foliar material of various C and N concentrations previously analysed in Jena.

3.6 Cation and phosphorus determinations

In the Jena laboratory about 100 mg of sample material was first submitted to a microwave-assisted high pressure digestion (Multiwave, Anton Paar, Graz, Austria) after addition of 3 ml of 65% HNO_3. Maximum reaction temperature was 230 °C with maximum pressures of 25–30 bar. To check for possible contamination of reagents and vessels, a blank was run with each series of standard reference materials or samples. After digestion, blank solutions and samples (reference materials and plant samples) were transferred to 50 ml glass vessels which were filled to the mark with ultrapure water (Millipore, Eschborn, Germany) and analysed by ICP-OES (Model Optima 3300 DV, Perkin Elmer, Norwalk, CT, USA) with a 40 MHz, free-running RF-Generator and an array detector allowing for the simultaneous determination of the elements using wavelengths as given in Boumans (1987) and DIN EN ISO 11885 (1998). In the Manaus laboratory, concentrations of P, K, Ca and Mg were determined after digestion with a nitric/perchloric acid mixture as described in detail by Malavolta et al. (1989). Concentrations of K, Ca and Mg in the extracts were subsequently determined using an Atomic Absorption Spectrophotometer (Model 1100b, Perkin Elmer, Norwalk, CT, USA) as prescribed by Anderson and Ingram (1993). Phosphorus was determined by colorimetry (Olsen and Sommers, 1982) using a UV visible spectrophotometer (Model 1240, Shimadzu, Kyoto, Japan). As for the Jena laboratory, to check for possible contamination of reagents and vessels, a blank was run with each series of standard reference materials or samples. Intercalibration between the two laboratories was achieved by the use of the same external and internal standards as for C and N (Sect. 3.5).

3.7 Carbon isotope determinations

In the Jena laboratory, $^{13}C/^{12}C$ isotopes were measured as described in Werner and Brand (2001). In short: within the same sequence of analyses, bulk tissue samples, laboratory reference materials (including quality control standards) and blanks were combusted quantitatively using an NA 1110 elemental analyser equipped with an AS 128 autosampler (CE Instruments, Rodano, Italy) attached to a Delta-C isotope ratio mass spectrometer (Thermo-Finnigan MAT, Bremen, Germany) using a ConFlo III interface (Werner et al., 1999). In the CENA laboratory, Brazilian samples were analysed as described in Ometto et al. (2006). In brief, 1–2 mg of sample was combusted in an elemental analyser (CE Instruments, Rodano, Italy) coupled to an isotopic ratio mass spectrometer (IRMS Delta Plus, Thermo-Finnigan MAT, San Jose CA, USA) operating in continuous flow mode.

Inter-calibration exercises between MPI-BGC and CENA using secondary standards and other plant material showed small but significant and systematic differences between the two laboratories (r^2=0.99). These have been corrected for here with results from the CENA laboratory adjusted to provide full isotope scale equivalence with the MPI-BGC results.

4 Statistical analysis

As we were interested in vertical variations in foliar characteristics with individual trees and variations in these characteristics between individual trees as a function of canopy height (and not so much concerned with plot-to-plot variations – these are considered in Fyllas et al., 2009) we used multilevel modelling techniques (Snijders and Bosker, 1999) treating both tree-to-tree variation (within a plot) and variations in overall mean values (between plots) as random (residual) effects. The Basin-wide average within- and between-tree gradients was thus determined according to

$$\Theta_{\ell tp} = \beta_{0tp} + \beta_1 h_{\ell tp} + \beta_2 h_c + R_{\ell pt}, \quad (4)$$

where $\Theta_{\ell tp}$ can be taken to represent any physiological parameter of interest (measured on leaf "ℓ" within tree "t" located within plot "p"), β_{0tp} is an intercept term which, as indicated by its nomenclature, is allowed to vary both between trees and between individual plots, β_1 is a coefficient that describes how Θ varies with the height at which it was sampled (common to all leaves, trees and plots), β_2 is an additional coefficient describing how $\Theta_{\ell tp}$ varies with mean tree canopy height, h_c, and $R_{\ell tp}$ is a residual term.

The tree and plot dependent intercepts can be split into an average intercept and group dependent deviations. Firstly we write

$$\beta_{0tp} = \delta_{00p} + U_{0tp}, \quad (5)$$

where δ_{00p} is the average intercept for the trees sampled within each plot and U_{0tp} is a random variable controlling

for the effects of variations between trees (i.e. with a unique value for each tree within each plot). Likewise, we also write

$$\delta_{00p} = \gamma_{000} + V_{00p}, \quad (6)$$

where γ_{000} is the average intercept for the entire dataset and V_{00p} is a random variable controlling for the effects of variations between each plot (i.e. with a unique value for each plot). Using a general notation then, we can combine Eqs. (4–6) to yield

$$\Theta_{ltp} = \gamma_{000} + \gamma_{100}h_{\ell t} + \gamma_{010}h_c + V_{00p} + U_{0tp} + R_{\ell tp}, \quad (7)$$

where γ_{100} describes how variations in Θ between leaves within a tree vary with canopy height (with the same value for all trees within all plots) and γ_{010} is a between-tree regression coefficient that describes how Θ varies with the overall (mean) canopy height for each tree (with the same value applying to all trees within all plots). For the V_{00p} and U_{0tp}, just as is the case for the $R_{\ell tp}$, it is assumed they are drawn from normally distributed populations and the population variance of the lower level residuals ($R_{\ell t}$) is likewise assumed to be constant across trees. Note that within each plot the mean value of $U_{0tp} \equiv 0$ and likewise the weighted mean value of $V_{0tp} \equiv 0$ for the dataset as a whole. As is the normal case in any regression model, for each tree the mean $R_{\ell tp} \equiv 0$.

Equation (7) is a "three-level random intercept model" with leaves (level 1) nested within trees (level 2) which are themselves nested within plots (level 3). Associated with the three residual terms there is variability at all three levels and we denote the associated variances as

$$\mathrm{var}(R_{\ell tp}), = \sigma^2, \ \mathrm{var}(U_{0tp}) = \tau^2, \ \mathrm{var}(V_{00p}) = \phi^2. \quad (8)$$

The total variance between all leaves is $\sigma^2+\tau^2+\phi^2$ and the population variance between trees is $\tau^2+\phi^2$.

Equation (7) is flexible in that the within-tree regression coefficient is allowed to differ from the between-tree regression coefficient. In analogy with the two-level model derivation in Chap. 4 of Snijders and Bosker (1999) and considering the terms within a given tree, these terms can be reordered as

$$\Theta_{\ell tp} = (\gamma_{000}+\gamma_{010}h_c+U_{0tp}+V_{00p})+\gamma_{100}h_{\ell tp}+R_{\ell tp}. \quad (9)$$

The random part between the parenthesis is the intercept for this tree and the regression coefficient for variation of Θ with height within trees is γ_{100}. The systematic (non-random) part is the within-tree regression line

$$\Theta_{\ell tp} = (\gamma_{000} + \gamma_{010}h_c) + \gamma_{100}h_{\ell tp}. \quad (10)$$

On the other hand, considering only the relationship between the average value of Θ within a canopy and the average canopy height, h_C, then Eq. (9) becomes

$$\Theta_{.tp} = \gamma_{000} + \gamma_{010}h_c + \gamma_{100}h_c + V_{00p} + U_{0tp}, \quad (11)$$

and the systematic part of the model can then be written as

$$\Theta_{.tp} = \gamma_{000} + (\gamma_{010} + \gamma_{100})h_c. \quad (12)$$

This shows that the between-tree regression coefficient in the random intercept model is $\gamma_{010}+\gamma_{100}$. Thus, when the relationship between any parameter Θ and height is different for between-tree as opposed to within-tree variation in the analysis which follows then this means γ_{010} is significantly different from zero. Where this is not the case, any variation in Θ with height is of a statistically similar magnitude irrespective of whether or not the source of variation is sampling at different heights within the one tree or comparing the average values for trees of different heights.

All analyses were undertaken with the *MLwinN* software package (Rabash et al., 2004). Heights were centered according to the mean tree height for the dataset (19.8 m) so the intercept estimates (γ_{000}) given represent the estimated value of each Θ at that height.

5 Results

5.1 Sources of variation

In order to examine the inherent sources of variability in the dataset, we first fitted a "null model" to untransformed data according to

$$\Theta_{\ell tp} = \gamma_{000} + V_{00p} + U_{0tp} + R_{\ell tp}. \quad (13)$$

From this model and Eq. (8) the contribution of variations within and between trees and plots to the overall variance within the dataset can be simply apportioned and the results are shown in Fig. 5. This shows that, without exception (using the subscript "DW" to denote concentrations are here being expressed on a dry-weight basis), the variability observed in the eight Θ examined *viz.* M_A and $\delta^{13}C$, $[N]_{DW}$, $[P]_{DW}$, $[C]_{DW}$, $[Ca]_{DW}$, $[K]_{DW}$ and $[Mg]_{DW}$ was greater between trees than the variance associated with the sampling of the three different heights within trees. Moreover, with the notable exception of $[P]_{DW}$, the between-plot variance was also generally less than the within-plot variance, the latter being associated with tree-to-tree variations within individual plots.

5.2 Vertical profiles

The underlying raw data giving rise to Table 1 and used in the subsequent multilevel analysis is shown in Fig. 6, with a different colour coding for the different regions. This "Jackson Pollock Plot" shows that, although there is considerable variability in the data, certain patterns exist. For example, on average there is a trend for an increase in M_A with increasing height and the opposite is the case for $\delta^{13}C$. On the other hand, generally speaking, concentrations in $[N]_{DW}$ and $[P]_{DW}$ are quite consistent within a given tree, although there are of course exceptions, especially at higher concentrations. Foliar carbon varies substantially between trees, and close examination shows that although usually very consistent within a given tree, there is often a slight tendency

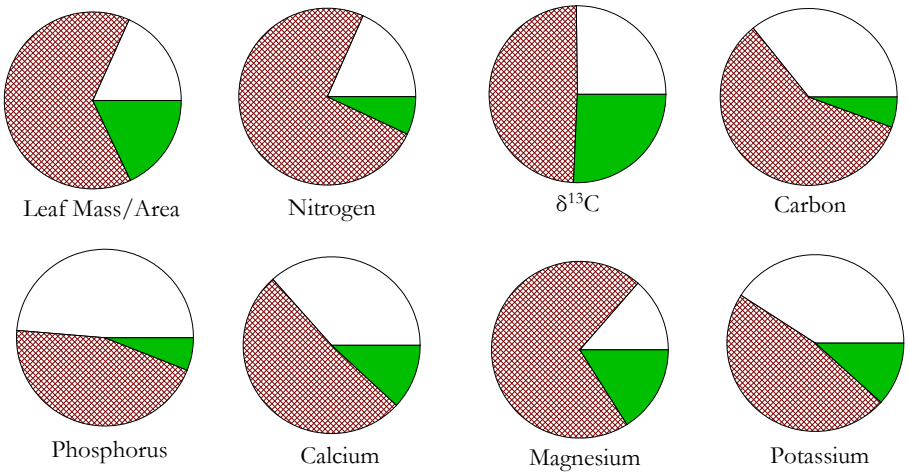

Fig. 5. Partitioning of the observed variance in the dataset according to Eq. (13). Green = variability with height within individual trees; purple hatches; variability between trees within individual plots; white = variability between plots.

for $[C]_{DW}$ to increase with height. Variations in $[Mg]_{DW}$ were similar to $[Ca]_{DW}$ and $[K]_{DW}$ with no strong trend with height readily apparent.

From Fig. 6 it can be seen that there is considerable heteroscedastity in the data with the variance of the dependent variables tending to increase with their absolute value but not with the value of the independent (height) variable. This was the case for all Θ except maybe $[C]_{DW}$ and $\delta^{13}C$. Moreover, an examination of residual variances showed marked departures from normality, even when plot-to-plot differences in overall mean values were taken into account. We therefore transformed all data (taking the absolute value of $\delta^{13}C$) prior to analysis, fitting the equation

$$\log_e(\Theta_{\ell tp}) = \gamma_{000}+\gamma_{100}h_{\ell t}+\gamma_{010}h_c+V_{00p}+U_{0tp}+R_{\ell tp}. \quad (14)$$

Noting that due to the logarithmic transform of the $\Theta_{\ell tp}$, terms, the height coefficients in Eq. (14) (γ_{10} and γ_{01}) now refer to the proportional changes in the $\Theta_{\ell tp}$ with $h_{\ell t}$ and h_C per metre respectively, results are listed in Table 1. Here the null hypothesis that a certain regression parameter (γ_h) is zero (i.e. H_0: γ_h=0) can be tested according to a two tailed *t*-test, T, $(\gamma_h)=\hat{\gamma}_h/[\text{S.E.}(\hat{\gamma}_h)]$, the so called *Wald test*. This indicates (as shown in bold font) that within tree canopy gradients were significantly different to zero only for M_A, $[C]_{DW}$, $\delta^{13}C$ and $[Mg]_{DW}$. From Eq. (12), the parameter γ_{010} can be taken to reflect the difference between the within-tree and between-tree slopes and a separate Wald test can be used to determine if the overall coefficient for the between-tree coefficient ($\gamma_{100}+\gamma_{010}$) is significantly different from zero (Snijders and Bosker, 1999). From such an analysis we conclude

1. The between-tree coefficient for M_A is not significantly different to the within tree coefficient ($P\leq 0.05$). Both are significantly different to zero ($P\leq 0.05$) with M_A increasing with increasing height.

2. There is no detectable within-tree gradient for $[N]_{DW}$, $[P]_{DW}$ or $[Ca]_{DW}$. Nor is there any significant overall tendency for mean canopy $[N]_{DW}$ or $[P]_{DW}$ concentrations to increase with mean tree canopy height ($P\geq 0.10$).

3. Foliar $|\delta^{13}C|$ decreases with height irrespective of whether the source of variation is within-tree or between-tree. That is to say, taller trees have less negative $\delta^{13}C$ than shorter trees and higher leaves also tend to have less negative $\delta^{13}C$ than those lower down within the same tree. The gradients with height are similar for both sources of variation and are both significantly different from zero ($P\leq 0.05$).

4. There is a significant tendency for $[C]_{DW}$ to increase with height within an individual tree, and also for taller trees to have a higher foliar C content ($P\leq 0.05$).

5. Although there is a significant tendency for $[Mg]_{DW}$ to decrease with increasing height within a given tree ($P\leq 0.05$), no such pattern is observed for the variation in $[Mg]_{DW}$ between trees with $(\gamma_{100}+\gamma_{010})/[\text{S.E.}(\hat{\gamma}_{h_C})]$ $T_{0.10}$. Potassium also shows a significant tendency to decrease with increasing height within a given tree ($P\leq 0.05$). Contrary to magnesium, this effect persists, or is perhaps even amplified when tree-to-tree variation is additionally considered.

Figure 7 shows the fitted slopes and the data, in all cases normalised to the fitted value for each tree at the average sampling height of 19.8 m. Here a comparison of the plots for within-tree and between-tree variation show the generally similar increases for M_A with height and decreases in $\delta^{13}C$ and $[C]_{DW}$ with height, irrespective of the source of variation. On the other hand, the much steeper gradient for $[K]_{DW}$

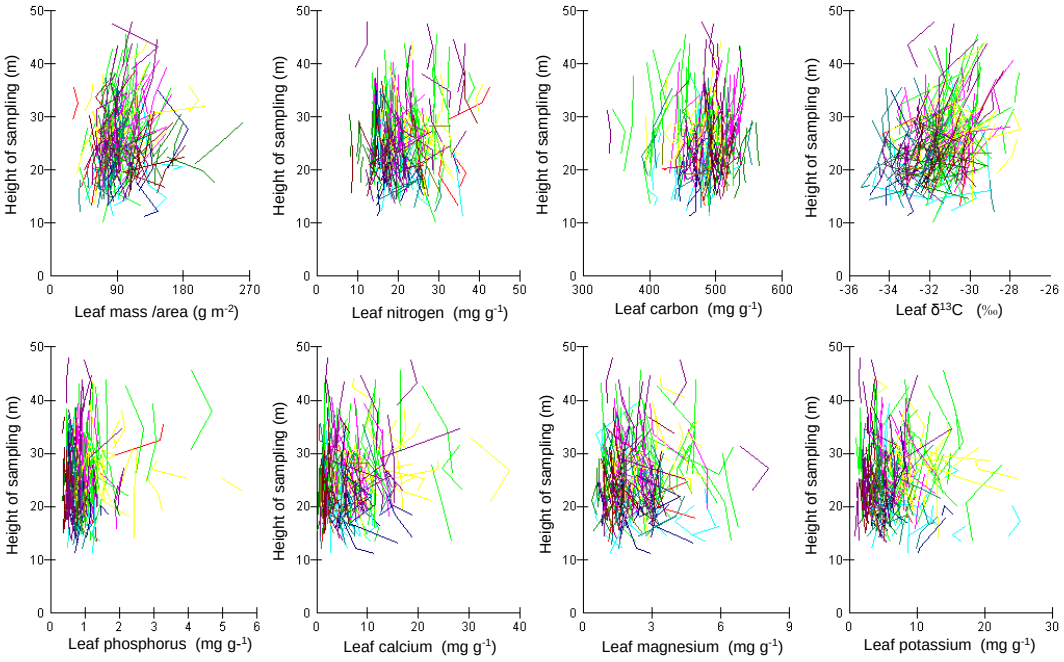

Fig. 6. Vertical gradients in leaf mass per unit area, $[N]_{DW}$, leaf $[C]_{DW}$, $\delta^{13}C$, $[P]_{DW}$, $[Ca]_{DW}$, $[Mg]_{DW}$ and $[K]_{DW}$ for 204 trees sampled across Amazonia. Different colours refer to different regions.

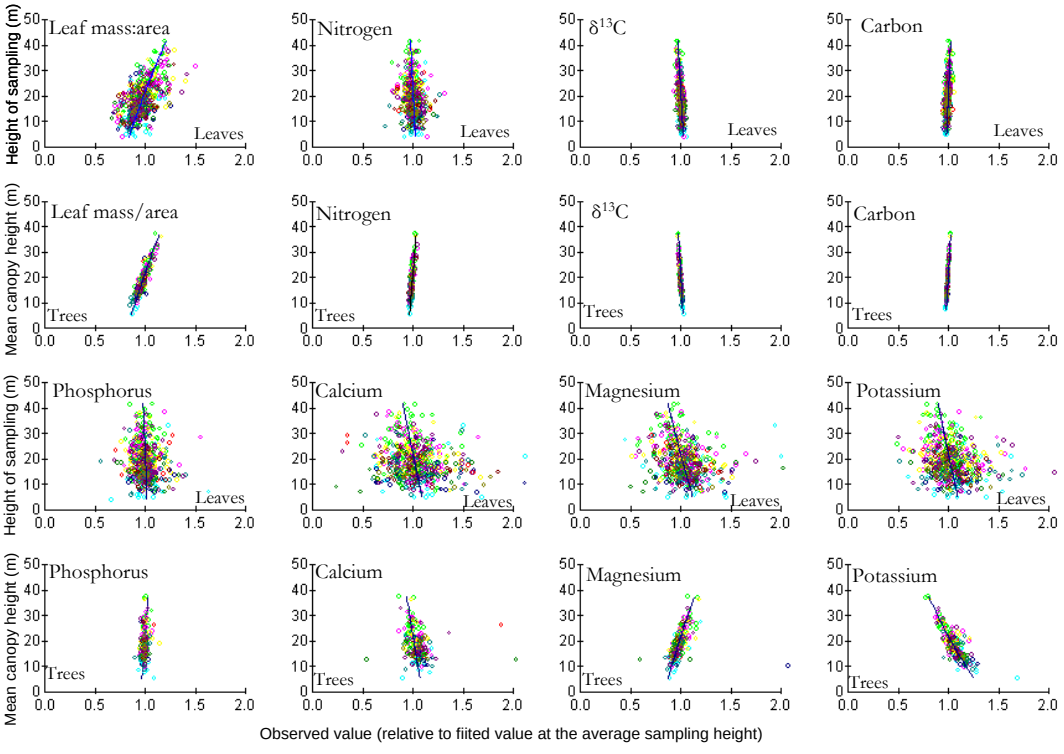

Fig. 7. Observed values and fitted lines for within-tree gradients ("Leaves") and tree-to-tree gradients ("Trees") for leaf mass per unit area, $[N]_{DW}$, $[C]_{DW}$, $\delta^{13}C$, $[P]_{DW}$, $[Ca]_{DW}$, $[Mg]_{DW}$ and $[K]_{DW}$ for 204 trees sampled across Amazonia. Different colours refer to different regions.

Table 1. Estimated intercept and coefficients according to Eq. (14) for leaf mass per unit area, leaf [N], leaf [C], leaf δ^{13}C, leaf [P], leaf [Ca], leaf [Mg] and leaf [K] all expressed on a leaf dry weight basis. Significant values (P≤0.05) are shown in bold.

	Log_e [Leaf mass/area] (g m^{-2})		Log_e [Nitrogen] (mg g^{-1})		$\text{Log}_e\lvert\delta^{13}\text{C}\rvert$ (‰)		Log_e [Carbon] (mg g^{-1})	
Fixed effect	Coefficient	S. E.	Coefficient	S. E.	Coefficient	S. E.	Coefficient	S. E.
γ_{000}= Intercept	4.560	0.0270	3.004	0.0267	3.673	0.0032	6.185	0.0077
γ_{100}= Coefficient of h	**0.00981**	**0.00123**	−0.00121	0.00081	**−0.00151**	**0.00019**	**0.00114**	**0.00018**
γ_{010}= Coefficient of (h_C-h)	0.00104	0.00354	0.00332	0.00329	0.00013	0.00048	0.00036	0.00082
Random Effect	Parameter	S. E.	Parameter	S. E.	Parameter	S. E.	Parameter	S. E.
φ_0^2= between plot variance	0.01693	0.00689	0.01783	0.00689	0.00026	0.00009	0.00201	0.00058
τ_0^2= between-tree variance	0.06047	0.00757	0.05876	0.00711	0.00747	0.00010	0.00334	0.00041
σ_0^2= within tree variance	0.01382	0.00099	0.00611	0.00044	0.00033	0.00002	0.00028	0.00003
	Log_e [Phosphorus] (mg g^{-1})		Log_e [Calcium] (mg g^{-1})		Log_e [Magnesium] (mg g^{-1})		Log_e [Potassium] (mg g^{-1})	
Fixed effect	Coefficient	S. E.	Coefficient	S. E.	Coefficient	S. E.	Coefficient	S. E.
γ_{000}= Intercept	−0.1244	0.0508	1.532	0.098	0.6991	0.0485	1.646	0.070
γ_{100}= Coefficient of h	−0.00107	0.00130	−0.00520	0.00320	**−0.00684**	**0.00218**	**−0.00538**	**0.00220**
γ_{010}= Coefficient of (h_C-h)	0.00206	0.00460	0.00106	0.00937	**0.01490**	**0.00642**	−0.00853	0.00604
Random Effect	Parameter	S. E.	Parameter	S. E.	Parameter	S. E.	Parameter	S. E.
φ_0^2= between plot variance	0.10919	0.02691	0.41396	0.09744	0.05785	0.02232	0.22444	0.04989
τ_0^2= between-tree variance	0.09322	0.01150	0.30900	0.04009	0.18150	0.02292	0.12120	0.01604
σ_0^2= within tree variance	0.01519	0.00109	0.09229	0.00663	0.04282	0.00307	0.04371	0.00314

when between-tree variations are considered is also apparent as is a strong contrast in directions for $[\text{Mg}]_{\text{DW}}$. Taller trees tend to have slightly higher $[\text{Mg}]_{\text{DW}}$, but within individual trees $[\text{Mg}]_{\text{DW}}$ declines with increasing height. Though not significant, the trends for slightly decreased $[\text{N}]_{\text{DW}}$ and $[\text{P}]_{\text{DW}}$ with height in individual tree canopies can also clearly be seen. Note that because all values are normalised to that of the fitted value at the average sampling height, the tree-to-tree variations appear in this graph to be much less than for the actual data themselves (see Fig. 6).

5.3 Area based profiles

Vertical variations in foliar nitrogen and/or phosphorus concentrations within plant canopies can be expected to substantially affect photosynthetic rates which are normally expressed per unit leaf area (Carswell et al., 2000; Domingues et al., 2005; Mercado et al., 2009; Domingues et al., 2010). It was thus also of interest to examine vertical gradients within and between trees also expressing nutrients on a leaf area basis (Table 2) – this simply being calculated as the product of the nutrient concentration (DW basis) and M_{A}, and with area based concentrations here identified by an "A" subscript. When done, this shows similar and significant within-tree positive gradients to exist for both $[\text{N}]_{\text{A}}$ and $[\text{P}]_{\text{A}}$. The between-tree gradients are in both cases about 50% steeper than the within-tree gradients, but this difference is not statistically significant. The negative gradient in $[\text{C}]_{\text{A}}$ as on a DW basis is maintained, as is the positive gradient for $[\text{K}]_{\text{A}}$, though in the case of $[\text{K}]_{\text{A}}$ the between-tree gradient is no longer statistically stronger than observed within individual trees. The pattern for magnesium is also very different on leaf-area versus dry-weight basis. The negative DW gradient (lower values higher up in the canopy) is counterbalanced by the positive gradient in M_{A} meaning that within individual tree canopies no gradient in $[\text{Mg}]_{\text{A}}$ exists. On the other hand, the positive between-tree gradient in magnesium is amplified when expressed on an area basis, with taller trees having significantly higher $[\text{Mg}]_{\text{A}}$ than their shorter counterparts.

Gradients for $[\text{N}]_{\text{A}}$ and $[\text{P}]_{\text{A}}$ are shown in Fig. 8, again with each tree having its value normalised to the fitted value at the average sampling height of 19.8 m. This illustrates the similar overall patterns observed for $[\text{N}]_{\text{A}}$ and $[\text{P}]_{\text{A}}$, a result that is not surprising as a comparison of Fig. 8 with Fig. 7 in conjunction with Tables 1 and 2 shows that almost all the variation observed in $[\text{N}]_{\text{A}}$ and $[\text{P}]_{\text{A}}$; both within and between trees, is due to the increase in M_{A} with height with $[\text{N}]_{\text{DW}}$ and $[\text{P}]_{\text{DW}}$ staying more or less constant within a given tree and also showing no systematic variation with h_{C} when different trees within the one stand are compared.

Table 2. Estimated intercept and coefficients according to Eq. (14) for leaf [N], leaf [C], leaf [P], leaf [Ca], leaf [Mg] and leaf [K], all expressed on a leaf area basis. Significant values (P≤0.05) are shown in bold.

	Log_e [Nitrogen] (mg m^{-2})		Log_e [Carbon] (mg m^{-2})		Log_e [Phosphorus] (mg m^{-2})	
Fixed effects	Coefficient	S. E.	Coefficient	S. E.	Coefficient	S. E.
γ_{000}= Intercept	7.572	0.021	10.75	0.011	4.448	0.0475
γ_{100}= Coefficient of h	**0.00873**	**0.00136**	**−0.01112**	**0.00135**	**0.00893**	**0.00167**
γ_{010}= Coefficient of ($h_C - h$)	0.00372	0.00351	0.00066	0.00426	0.00465	0.00398
Random Effects	Parameter	S. E.	Parameter	S. E.	Parameter	S. E.
φ_0^2= between plot variance	0.00215	0.00463	0.02856	0.01155	0.09834	0.02210
τ_0^2= between-tree variance	0.05775	0.00773	0.06670	0.00850	0.05822	0.00782
σ_0^2= within tree variance	0.01642	0.00135	0.01521	0.00119	0.02460	0.00226
	Log_e [Calcium] (mg m^{-2})		Log_e [Magnesium] (mg m^{-2})		Log_e [Potassium] (mg m^{-2})	
Fixed effects	Coefficient	S. E.	Coefficient	S. E.	Coefficient	S. E.
γ_{000}= Intercept	6.126	0.0979	5.268	0.0498	6.232	0.07187
γ_{100}= Coefficient of h	0.00372	0.00234	0.00264	0.00244	**0.004425**	**0.00223**
γ_{010}= Coefficient of ($h_C - h$)	−0.00156	0.00654	**0.01712**	**0.00700**	−0.00155	0.00654
Random Effects	Parameter	S. E.	Parameter	S. E.	Parameter	S. E.
φ_0^2= between plot variance	0.3553	0.0915	0.05574	0.02276	0.3553	0.09146
τ_0^2= between-tree variance	0.3867	0.0538	0.18610	0.02458	0.3867	0.05381
σ_0^2= within-tree variance	0.1072	0.0072	0.05135	0.00388	0.1072	0.00721

5.4 Do tree-to-tree variations in within-canopy gradients exist?

The analysis so far has assumed that for all Θ the within-tree gradients are the same for all plots and trees, but that different plots and the trees within them may assume different overall nutrient concentrations (a "random intercept model") But, especially in light of the model results of Sect. 2 which suggest that trees with the highest photosynthetic capacity should have the highest within canopy extinction coefficients, it was also of interest to determine if gradients observed differed between trees, and if so, in a systematic way. Given the "noise" apparent in Fig. 6, this was obviously not an easy question to answer, but it was attempted by taking $\beta_{1tp}=\gamma_{100}h_{\ell tp}+U_{1tp}h_{\ell tp}$ (see Eq. 4), this then adding an additional random term to Eq. (7) *viz.*,

$$\Theta_{\ell tp} = \gamma_{000} + \gamma_{100}h_{\ell tp} + \gamma_{010}h_c + V_{00p} + U_{0tp} + U_{1tp}h_{\ell tp} + R_{\ell tp}. \quad (15)$$

The additional term allows different trees to have different within-canopy gradients – a so called "random slope model" (Snijders and Bosker, 1999) with a χ^2 test then employable to see if the model fit has been improved. And indeed, when this was attempted, it was found that significant tree-to-tree variations in within canopy gradients were observed (P≤0.05), but only for M_A, $|\delta^{13}C|$ and P_A. Moreover, as is shown in Fig. 9 these variations in slopes (or "extinction coefficients") were not random, but inter-related and correlated with the mean M_A, $|\delta^{13}C|$ and $[P]_A$ of the trees concerned. In particular, tree-to-tree variation in all three of the above parameters were well correlated with mean canopy $[P]_A$, this being the average of all three measurements taken on each tree, and denoted here as $\langle[P]_A\rangle$. The very similar patterns for the gradients in M_A and $[P]_A$ with $\langle[P]_A\rangle$ suggests that most of the between-tree variability in within canopy gradients in $[P]_A$ was due to variations in M_A rather than $[P]_{DW}$. The strong decline in $|\delta^{13}C|$ with increasing $\langle[P]_A\rangle$ is also of note, suggesting that variations in photosynthetic ^{13}C discrimination within tropical tree canopies are intricately linked with plant metabolic processes.

6 Discussion

6.1 Gradients in nitrogen, phosphorus and photosynthetic capacity

That plants can acclimate to different irradiances at chloroplast, leaf and canopy level has long been appreciated (Monsi and Saeki, 1953; Boardman, 1977; Björkman, 1981) and a key focus of recent years has been understanding the way plants that allocate their resources throughout their canopies, with one main emphasis being the extent to which observed distributions serve to maximise photosynthetic carbon gain (Niinemets, 2007). It was Field (1983) who first proposed

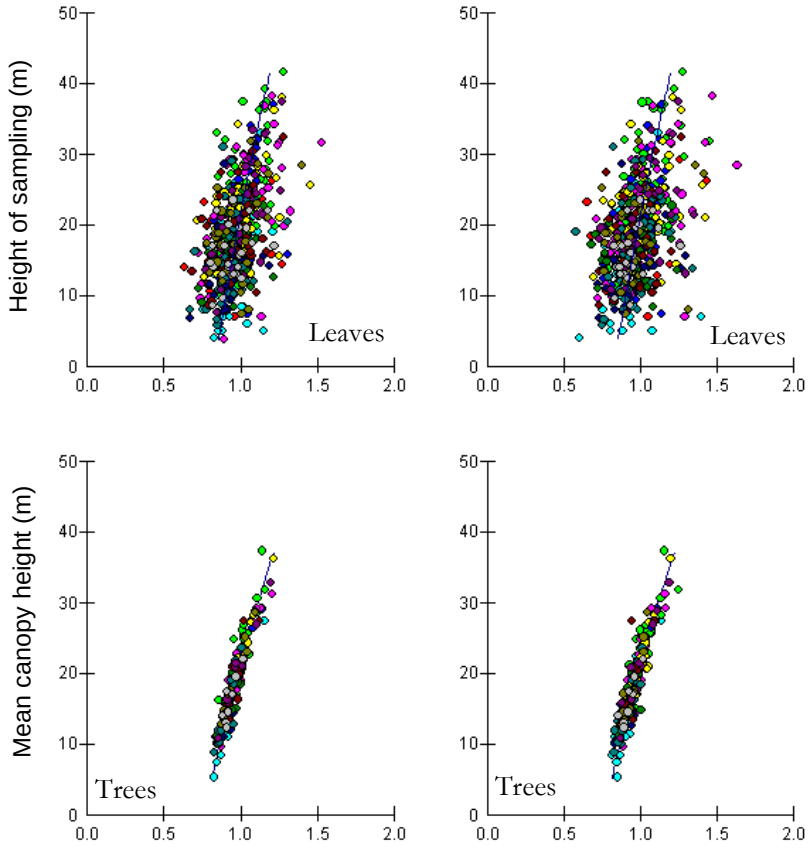

Fig. 8. Vertical gradients in leaf [N], and leaf [P] expressed on a leaf area basis. Different colours refer to different regions.

that plant photosynthetic carbon gain would be optimized if key physiological resources required for photosynthesis (in his case nitrogen) were allocated in direct proportion to the average Q received. Especially when considered in conjunction with the mathematical simplicities that ensue (Farquhar, 1989) this idea of "optimization" is conceptually attractive, even being incorporated into some canopy gas exchange models (Lloyd et al., 1995; Sands, 1995; Sellers et al., 1996). But it is also now clear that although the decline in photosynthetically important elements such as nitrogen and phosphorus within plant canopies can be considerable, and sometimes even impressive, this decline is never to the same extent that it matches the reduction in Q (De Jong and Doyle, 1985; Carswell et al., 1980; Meir et al., 2002; Anten, 2005; Wright et al., 2006; see also supplementary information: http://www.biogeosciences.net/7/1833/2010/bg-7-1833-2010-supplement.pdf).

As to why this should be so has proved somewhat of an enigma, it being generally accepted that natural selection should have resulted in plants optimising their resource strategies. Various hypotheses have been proposed to account for this apparent "non-optimality". These include that plants do not grow as isolated individuals but rather in competition with others (Anten, 2005), that it might be related to direct versus diffuse radiative transfer (Buckley et al., 2002; Alton and North, 2007) or not all nitrogen being related to photosynthesis (Hikosaka, 2005); that there may be optimisation of N to light gradients within leaves as well as canopies (Terashima et al., 2005); that the required very high nitrogen concentrations at the top of the canopy may place leaves at strong risk of herbivory (Stockhoff, 1994); that there may be considerable costs of retranslocating nutrients within the plant (Field, 1983; Wright et al., 2006), that plants may over invest in Rubisco in order to cope with temporal variabilities in their environment (Warren et al., 2000) and, especially as gradients in nutrients and photosynthetic capacity are generally driven by gradients in M_A rather than by variations in dry-weight nutrient concentrations (Reich et al., 1998; Ellsworth and Reich, 1993; Evans and Poorter, 2001), that there may be a practical lower limit to the minimum M_A and hence N_A that any species can achieve (Meir et al., 2002).

Although with some affinity with the latter suggestion, and the observation of both Pons et al. (1989) and

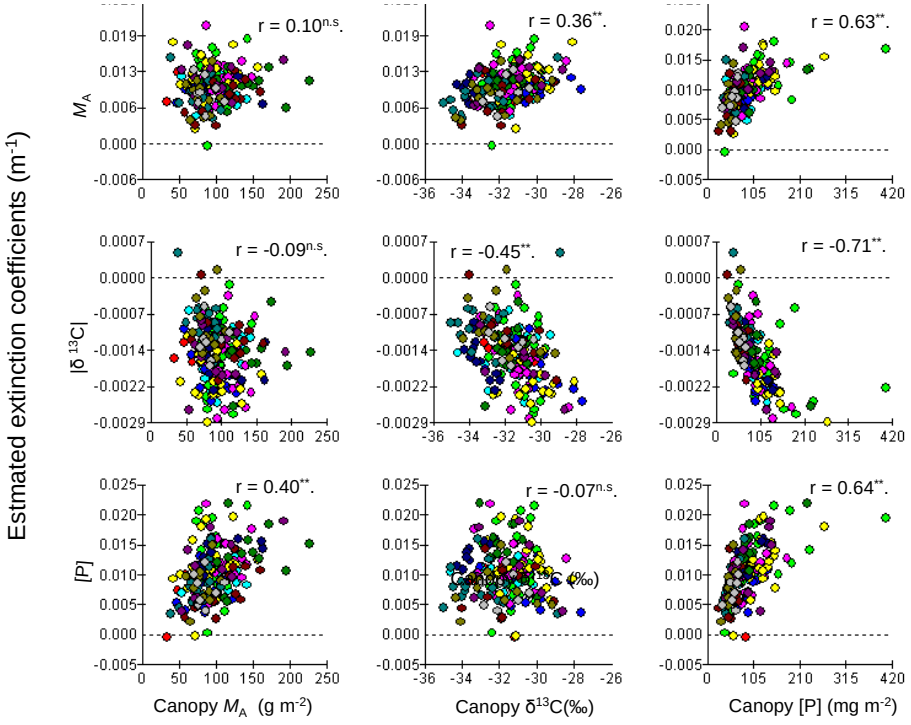

Fig. 9. Relationship between within canopy gradients in leaf mass per unit area (M_A), foliar $\delta^{13}C$ and leaf phosphorus concentrations (area basis) and the overall mean M_A $\delta^{13}C$ and $[P]_A$ in the same tree. Also shown are Spearman's rank correlation coefficients and their level of significance (*; $P<0.05$; **; $P<0.01$). Different colours refer to different regions.

Hollinger (1996) that there may be practical limits to A_{max} for any given species, the answer we present to this long standing apparent discrepancy differs somewhat to other suggestions made to date. That is to say, we believe the optimality question has actually been incorrectly posed. And we suggest from our simulations and results presented in Sect. 2 that once correctly posed, it turns out gradients of photosynthetic resources within plant canopies are, in fact, close to optimal.

For example, in some cases it has simply been assumed that the problem is simply one of allocating resources for a canopy of a given leaf area index and photosynthetic capacity (as observed). But when this is done (e.g. dePury and Farquhar, 1997) what emerges are unrealistically high nutrient concentrations being required at the top of the canopy, inconsistent with the physiological tradeoffs that clearly exist in terms of leaf structure and function (Wright et al., 2004). This is similar to the point of Meir et al. (2002) already mentioned above, that there is probably also a realistic lower limit to the M_A and nutrient content that any species can attain.

It is now well established that different species have characteristically different values of fundamentally linked physiological properties such as M_A, $[N]_{DW}$ and $[P]_{DW}$. For example Fyllas et al. (2009) showed that much of the considerable variability in these properties occurring within individual sample plots (Fig. 5) is a consequence of species-to-species variations, this being closely linked to other aspects of their physiological strategy including leaf lifespans (Wright et al., 2004) and hydraulic characteristics (Santiago et al., 2004; Meinzer et al., 2008). Such species dependent differences in key foliar physiological properties are also linked to practical morphological and anatomical constraints such as variations in leaf and palisade layer thickness and exposure of mesophyll surface area to the intercellular airspaces (Kenzo et al., 2006). That is not to say, of course, that both within-species variability and the modulation of key physiological traits by the environment does not occur. Both clearly do (Specht and Turner, 2006; Fyllas et al., 2009). Nevertheless, that an individual species can only vary in such functional traits to a limited extent and with this being much less than the observed global range (and thus with finite species overlap occurring) is fundamental to current theories of functional plant ecology (e.g. Reich et al., 2003; McGill et al., 2006). It therefore seems reasonable to argue that the question of optimisation within plant canopies should also be viewed within the constraints of these known physiological boundary conditions such as the maximum (species dependent) photosynthetic potential of the leaves at the top of the canopy. In some cases, the practical minimum value achievable at the bottom of the canopy may also be important, this

perhaps being structural (as suggested by Meir et al., 2002), or alternatively being a consequence of the need for all leaves to maintain a positive carbon balance once mature (Turgeon, 2006), as discussed in Appendix B.

One simple way to view the argument and it's consequences is through following the individual lines shown in Fig. 4. If A_0^* is kept constant, then a plant with an "optimal" distribution of its photosynthetic resources (high k_P) unavoidably has less total photosynthetic resource available to it than one that does not (low k_P). Thus, it is actually to a plant's advantage to have a shallow gradient in photosynthetic resources as this allows it to have a greater overall photosynthetic capacity (C_c) and hence a higher net rate of carbon gain, N_R. As discussed in Appendix B, it turns out there are several complexities which end up influencing the minimum k_P and maximum N_R which should occur, but nevertheless, the theory and model as presented here do lead to the (intuitive) prediction that plants with a low overall photosynthetic capacity should have shallower gradients in their photosynthetic resources than those with higher photosynthetic capacities. This can be inferred, for example, if we accept that phosphorus has a role in the photosynthetic process for tropical tress (Raaimakers et al., 1995; Lloyd et al., 2001; Domingues et al., 2010), from the relationship between $\langle[P]_A\rangle$ and the gradients shown in Fig. 9.

As is evidenced from Fig. 8 these tree-to-tree variations in the gradients of M_A and $[P]_A$ are also accompanied by correlated variations in $\delta^{13}C$. This suggests that for such trees compensating gradients in stomatal conductances do not necessarily occur (Rajendrudu and Naidu, 1997; Miyazawa et al., 2004) with leaves further down within the canopy having relatively higher ratios of intercellular to ambient CO_2 concentrations (c_i/c_a). Thus any gradient in overall photosynthetic rates may actually be less than that which would be inferred on the basis of nutrients (or photosynthetic capacity) alone. One reason for higher c_i/c_a for leaves lower down in tropical forest canopies may be the significantly lower leaf-to-air vapour pressure deficits which typically occur there (Shuttleworth, 1989). However, this does not readily explain why tree-to-tree variations in the magnitude of the gradient in $\delta^{13}C$ are so closely linked to variations in the gradients in M_A and $[P]_A$ (Fig. 9). This has been observed before for conifer trees by Duursma and Marshall (2006) and may be attributable to taller trees with higher than average high M_A and $[P]_A$ tending to occur in more exposed conditions and thus experiencing a greater likelihood of their upper canopy leaves being exposed to more severe water deficits during times of high insolation than those lower down (Niinemets et al., 2004). Consistent with this explanation is the less negative overall $\delta^{13}C$ for those trees with the sharpest gradients (Fig. 9).

The relationship of Fig. 9 is, interestingly, also consistent with greater differences between sun and shade leaves in M_A and many other leaf characteristics (including P_A) for gap-dependent species (as opposed to obligate-gap species or gap-independent species) as observed by Popma et al. (1992) for a tropical forest in Mexico. They found that gap-dependent species also had higher $\langle[N]_A\rangle$ and $\langle[P]_A\rangle$ than the other two species groups.

As well as increasing with height within trees, M_A also tended to be greater for taller trees within the same stand with $[N]_{DW}$ and $[P]_{DW}$ also showing similar patterns within and between different trees, *viz*. no significant gradient at all (Table 1, Fig. 7). Consequently, as was the case for within-tree variation, taller trees also tended to have higher $[N]_A$ and $[P]_A$ (Fig. 8). This has been reported before for $[N]_A$ and M_A in dipterocarp forests in Malaysia (Thomas and Bazzaz, 1999; Kenzo et al., 2006) with a tendency for taller trees to have a greater M_A being an apparently general phenomenon (Poorter et al., 2009). This phenomenon will be dealt with in more detail in an accompanying paper utilising a much larger additional data set of individual trees for which only upper-canopy leaves had been sampled. But suffice to say, it emerges that simple scaling relationships such as between M_A and $[N]_{DW}$ or $[P]_{DW}$ (Fyllas et al., 2009) are markedly improved when tree height is also considered as a covariable (S. Patiño et al., unpublished results).

6.2 Extrapolation to the stand level

As shown in Fig. 5, even when considering a study such as this encompassing sites across a wide range of soil substrates and climates within the Amazon Basin, the variability in nutrient concentrations, M_A, and $\delta^{13}C$ observed was mostly attributable to differences between trees within individual stands (plots). This is as opposed to being associated with the height of sampling within individual trees or even due to the trees being situated in different plots (see also the random error variances as listed in Table 1). This high within-plot heterogeneity has been noted before for tropical forest $[N]_{DW}$ and $[P]_{DW}$ (Townsend et al., 2008) and is attributable to the typically high species diversity of most of the plots sampled combined with the presence of substantial within- and between-species variations in nutrient concentrations (Fyllas et al., 2009). Combined with the typical complexities of tropical forest phyto-structure (e.g. Kellner et al., 2009) this then makes it virtually impossible to take relationships such as shown in Fig. 9 and somehow scale them up to estimate some sort of averaged stand level gradient. This is because one would not only need to know the relative abundances of the different trees with different characteristic nutrient concentrations, but also their individual height, canopy dimensions and the leaf area density distributions within their canopies.

But being able to predict such gradients is of critical importance, not only in the modelling of tropical forest carbon acquisition (Mercado et al., 2009), but also for simulations of terrestrial carbon exchange in general (Mercado et al., 2007).

In most studies attempting to simulate G_P, gradients in photosynthetic capacity are typically expressed in terms of

the cumulative L down from the top of the canopy (Hirose and Wegner, 1987; de Pury and Farquhar, 1995; Mercado et al., 2009) as is also the case for our simulations here in Sect. 2. In search of a general equation and also to further confirm one fundamental thesis here – that the magnitude of vertical gradients in photosynthetic capacity (expressed as an extinction coefficient) should scale with photosynthetic capacity (Sect. 2.3) – we have thus surveyed the literature, and attempted to estimate a form of k_P as in Eq. (A2) for as many broadleaf forests and/or trees as possible. As most terrestrial carbon exchange models utilise the activity of ribulose-1,5-bisphosphate carboxylase/oxygenase (Rubisco) for the uppermost leaves $V_{max(0)}$, as a critical input variable (e.g. Sellers et al., 1996) we have therefore attempted to also estimate this value from the same studies as is described in the Supplementary Information: http://www.biogeosciences.net/7/1833/2010/bg-7-1833-2010-supplement.pdf. In all, 18 profiles were identified and, when taken together, show a relationship between the within canopy extinction coefficient for Rubisco (k_V, per unit L) and $V_{max(0)}$ that is surprisingly good (Fig. 10) with a very strong positive relationship between $V_{max(0)}$ and k_V observed. This was despite the many assumptions required (see Supplementary Information: http://www.biogeosciences.net/7/1833/2010/bg-7-1833-2010-supplement.pdf) with associated uncertainties in the true values, and for which it should also be noted we have used a robust rank-based regression procedure (Terpstra and McKean, 2005) to avoid any overinfluence of outliers on the fitted line.

Especially as the range of k_V is virtually identical to that simulated for k_P in Fig. 4 this gives us increased confidence in the validity of the approach taken in Sect. 2 and, perhaps along with data from other vegetation types such as conifers and monocots, also suggests a way forward in terms of modelling photosynthesis at larger scales. According to the modelling study (Sect. 2) generally shallow gradients in photosynthetic capacity but with k_V increasing with upper leaf V_{max} can be interpreted as reflecting a likely optimisation of canopy carbon gain potential across a wide range of species with different photosynthetic capacities and geographic locations.

We also believe that previous schemes based on "big-leaf assumptions" also equating to optimality such as for Sellers et al. (1996), Haxeltine and Prentice (1996) and, of course, as also advocated by Lloyd et al. (1995), should probably now be abandoned. Indeed, it is interesting to note that, although a separate consideration of direct versus diffuse radiation may lead to improved model fits for canopy gas exchange models (e.g. Mercado et al., 2006), much of the effect attributed to the improved description of canopy light regime in the sun/shade model of de Pury and Farquhar (1997) was actually a consequence of their sun/shade model and multilayer model calculation using a k_V of ca. 0.3 rather than a value of more like 0.7 which is what a big-leaf model actually assumes (J. Lloyd, unpublished results). It may also be useful to note that that study and several others (e.g. Hirose and Werger, 1987) have used a slightly different paramaterisation of Eq. (A1) where the exponent is normalised by L. The two different mathematical forms give rise to very different results when L is allowed to vary. The latter form effectively changes the gradients in photosynthetic capacity throughout the entire plant canopy with any variation in L.

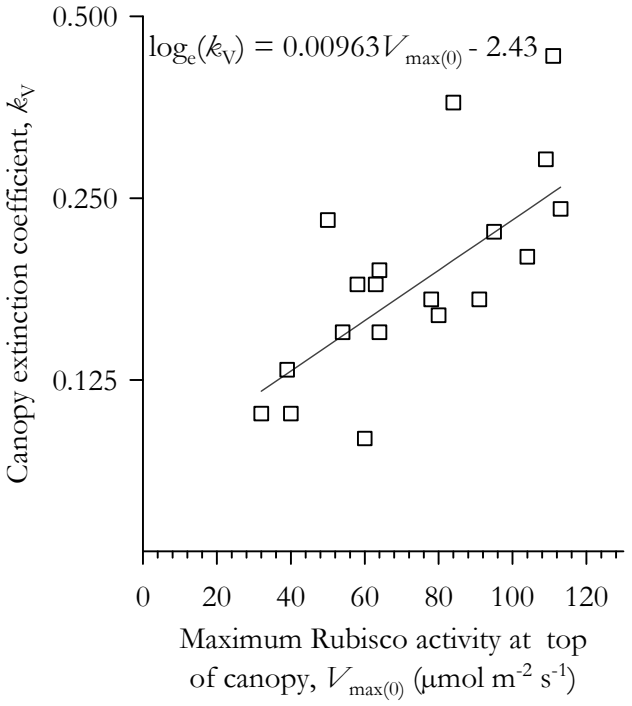

Fig. 10. Relationship between within canopy gradients in activity of ribulose-1,5, bisphosphate carboxylase/oxygenase, Rubisco, and maximum Rubisco activity in upper-canopy leaves for a range of broadleaf forests and/or trees taken from a literature review. Details of the individual studies and means of calculation are given in the Supplementary information. Note the logarithmic scale for k_V. Due to uncertainties in the estimates of both the independent and dependent variables from this literature survey (see Supplementary information), the fitted line has been obtained using a high breakpoint rank regression technique (Chang et al., 1999) and is significant at $P<0.01$.

6.3 Model and data uncertainties

Although the model described in Appendix A and utilised analytically in Sect. 2 does seem to be able to simulate L, G_P and k_P for Amazon forests, as well as making the general predication that within-canopy gradients should increase as does upper canopy photosynthetic capacity (Figs. 9 and 10), it should be emphasised that the model presented is more conceptual than quantitative. For example, it does not take into account effects of direct versus diffuse radiation (Buckley et al., 2002) and considers the forest canopy to consist only of one generic phenotype. This overlooks

the clear intra- and inter-species variations in photosynthetic characteristics and associated leaf traits that clearly occur, especially for tropical forest canopies (Domingues et al., 2005; Fyllas et al., 2009), along with substantial within and between-tree variations in leaf angle and size (Kitajima et al., 2005; Poseda et al., 2009) which should also give rise to attendant variations in k_I.

The model simulations also involve some simplistic assumptions regarding leaf lifetimes and associated annual construction costs of the photosynthetic machinery (Sect. 2.2). It ignores, for example, that shaded leaves lower down in the canopy may have much longer lifetimes than their sun-exposed counterparts (Lowman, 1992; Tong and Ng, 2008). We have also assumed an average leaf lifetime of one year, independent of M_A or A_{max}. Nevertheless, as mentioned already (Sect. 2.2), leaf lifetimes tend to correlate very poorly with A_{max} when the latter is expressed on a leaf area basis. And indeed, for Amazon forest trees, soil fertility seems to be able to strongly influence $[P]_{DW}$ without affecting M_A to any large degree (Fyllas et al., 2009). This suggests that the structural component of leaf longevity may be unlinked to concurrent changes in photosynthetic capacity when soil fertility is the primary source of variation – at least for tropical forest trees

Similarly, the carbon costs of nutrient acquisition which may be considerable (Lynch and Ho, 2005) have not been included in the calculations of Sect. 2.3. Effectively, if they were to be included (associated with variations in C_C), the optima in Fig. 4 would be shifted slightly to the left, with a less dramatic increase in N_R as C_C increases at low values, but with a more rapid decline at supra-optimal C_C.

Although not critical for the overall conclusions of the model, there are several assumptions regarding leaf respiratory costs which also involve uncertainties. For example, we have simply assumed that for all leaves $R_{(z)}$=0.08$A_{max(z)}$, even though this fraction has been reported to decline to some extent with depth within the canopy for tropical trees (Cavaleri et al., 2008). A slightly lower than modelled $R_{(z)}$ lower down within the canopy would effectively serve to make both the modelled optimal N_R and k_P to occur at slightly higher L in simulations such as shown in Fig. 3. Also important in this respect is that the model in Sect. 2 allows for significantly reduced leaf respiration rates in light at all but the lowest Q (Fig. A1a). The precise mechanism(s) and magnitude of this effect remain highly uncertain at the current time (Hurry et al., 2005). For the model described in Sect. 2, less inhibition at high Q than modelled would serve to reduce overall N_R and also make R_C less sensitive to changes in L as long as C_C remains constant, and thus with a slightly higher optimal L and k_P being simulated for any given C_C, but also with a lower N_R.

One further consideration is that variations in the construction and maintenance costs of foliar supporting tissues (twigs, branches and boles) have not been accounted for when allowing L to vary. Poorter et al. (2006) found crown area increasing more strongly with tree height than crown length. They interpreted this as suggesting that crown area expansion is the more efficient way to increase the number of apical meristems and leaf area,so as to occupy space, overshade neighbors, and reduce self-shading. Nevertheless, the nature of this relationship varies with tree developmental stage (Poorter et al., 2003, 2006) and, indeed, it does not necessarily follow that higher L trees need to be taller. This is because leaf area density within tropical tree crowns can also vary widely (Ashton, 1978) and thus a deep crown does not necessarily imply a high number of leaf layers. Moreover, taller trees also tend to have a lower bole wood density, as well as low density and weak branches, short branches, high resource costs per unit branch length, and low resource costs per unit stem length (Stark et al., 2006). Taken together, the above considerations suggest that the carbon construction costs of supporting tissue may not vary to any great degree (or systematically) with L and that their omission from the calculations of Sect. 2 is unlikely to have caused any significant error in the simulations or affected the basic conclusions reached.

The calculations undertaken for Fig. 10 (Sect. 6.2) as detailed in the Supplementary information: http://www.biogeosciences.net/7/1833/2010/bg-7-1833-2010-supplement.pdf have in many cases also required assumptions in the derivations of $V_{max(0)}$ and/or k_V. For example in the study of Ellsworth and Reich (1993) we have had to make assumptions about c_i, in order to estimate $V_{max(0)}$, also assuming it did not vary with canopy height. Also, as many studies have reported Q_z/Q_0 (see Eq. A2) rather than cumulative leaf area index, it was often necessary to make assumptions about k_I, for example as in Meir et al. (2002) – this being taken as uniform throughout the canopy, although it may also be the case that leaf angles, and hence k_I, may vary with canopy depth (Poseda et al., 2009). The required assumptions for each study are listed in the right hand column of Table S1 (Supplementary Information: http://www.biogeosciences.net/7/1833/2010/bg-7-1833-2010-supplement.pdf), and it is because of the considerable uncertainties involved with the estimates of both $V_{max(0)}$ and/or k_V that we have used a robust high breakpoint rank regression technique (Chang et al., 1999) to estimate the slope and its significance for the relationship shown in Fig. 10.

6.4 Gradients in carbon and cation concentrations

Gradients with height were observed in plant carbon concentrations, both within and between trees. Small within canopy gradients in $[C]_{DW}$ have been reported before by Poorter et al. (2006) who accounted for lower construction costs of low irradiance leaves in terms of lower levels of soluble phenolics. Studying upper-canopy leaves from across the Amazon Basin, Fyllas et al. (2009) also observed significant variations in foliar carbon content, relating this to variations in M_A

and the extent of investment in constitutive defenses. Consistent with this and the observed positive vertical gradient in $[C]_{DW}$ both between and within trees is the tendency for leaves higher up rain forest canopies to have greater levels of carbon based defense compounds (Lowman and Box, 1983; Downum et al., 2001; Dominy et al., 2003), this perhaps being associated with higher abundances of herbivores such as insects and other arthropods also occurring there (Sutton, 1989; Kato et al., 1995; Koike et al., 1998; Basset et al., 2001).

The decrease in $[Mg]_{DW}$ with height within individual trees (Table 1, Fig. 7) seems similar to that reported by Grubb and Edwards (1982) comparing saplings and mature trees within a New Guinea montane rain forest. They attributed this to the central role of Mg within the chlorophyll (Chl) complex (Shaul, 2002) with increased $[Chl]_{DW}$ for shaded leaves being a well documented phenomenon (Boardman, 1977; Björkman, 1981) – as generally seems to be also the case for tropical forest trees (Rozendaal et al., 2006). The within-tree Mg gradient was not, however, significant when expressed on a leaf area basis, despite both $[N]_A$ and $[P]_A$ declining with increasing canopy depth. Particularly for N, this is consistent with the idea that in shaded conditions a large portion of N is invested in chlorophyll for light capture, leading to high Chl:N ratios. On the other hand, for light exposed leaves a large proportion of N is invested in Rubisco with commensurate lower Chl:N ratios (Poorter et al., 2000; Evans and Poorter, 2001). By contrast $[Mg]_A$ did increase with height along with $[N]_A$ and $[P]_A$ when between-tree differences in tree height were the source of vertical variation (Table 2). Nevertheless, when comparing different rain forest trees $[Chl]_A$ seems to be independent of light environment or tree height (Rijkers et al., 2000). Probably then, this increase in $[Mg]_A$ with tree height relates to its other physiological functions, for example in the process of thylakoid acidification (Pottosin and Schönkmecht, 1996), as an activator of several photosynthetic enzymes including Rubisco (Gardemann et al., 1986; Portis, 1992) and as a ATP-cofactor required for phloem loading of sugars (Shaul, 1992). All these physiological functions would be expected to need to be proceeding at higher rates in taller trees with higher $[N]_A$ and $[P]_A$. This is because such trees would also most likely have higher photosynthetic rates by virtue of greater A_0^* (associated with higher $[N]_A$ and $[P]_A$: Domingues et al., 2010) as well as a greater probability of high light interception compared to trees occurring lower down the canopy stratum.

Potassium showed a different pattern to magnesium, with a decline in $[K]_{DW}$ with increasing height, both within- and between-trees (Table 2, Fig. 8). As potassium plays a key role in the maintenance of leaf osmotic potentials as well as being critical for stomatal function (Leigh and Wyn Jones, 1984; Lebaudy et al., 2008) this may appear counter-intuitive as, other things being equal, leaves higher up in the canopy should have both higher gas exchange rates (Carswell et al., 2000; Kenzo et al., 2006; Niinemets, 2007) and more negative osmotic potentials (Myers et al., 1987; Oberbauer et al., 1997; Niinemets et al., 1999; Niinemets and Valladares, 2004). Nevertheless, soluble carbohydrate concentrations are usually high for sun exposed leaves (Lichtenthaler et al., 1991; Gleason and Ares, 2004) with these sugars making a critical contribution to the required more negative osmotic potentials for the leaves higher up the canopy stratum (Niinemets and Valladares, 2004), perhaps also replacing potassium in this role to some extent (Leigh and Wyn Jones, 1984). It is also the case that leaf densities tend to be higher for high M_A leaves (e.g. Kenzo et al., 2006), mostly likely due to greater cell wall thicknesses (Syvertsen et al., 1995) and that associated with these high leaf densities are lower water contents (at saturation) per unit dry weight for high M_A leaves (Prior et al., 2004; Poorter et al. 2009) as well as a greater relative apoplastic water content (Oberbauer et al., 1987). Taken together, these observations mean that mesophyll protoplasmic volumes per unit dry weight should be substantially less for high M_A upper canopy leaves and thus any potassium present being relatively more effective as an osmoticum per unit foliar dry-weight.

7 Conclusions

This paper provides a new explanation as to why gradients in photosynthetic capacity within plant canopies are almost inevitably shallower than that of the light environment. This occurring despite the fact that simple optimization theory suggests that maximum plant carbon gain should be achieved when both gradients are identical. The argument is predicated on the observation, as already noted by others, that there is a practical limit to the maximum photosynthetic capacity a leaf can attain. The analysis here extends this notion through numerical simulation – showing that species with a high intrinsic maximum photosynthetic capacity should have sharper gradients than those with a lower CO_2 assimilation potential. This prediction is verified in two ways. First, it is shown for Amazon trees that variations in the magnitude of intra-canopy variations in phosphorus, a likely good surrogate for photosynthetic capacity, increase with the overall average concentrations of phosphorus (leaf area basis) for individual trees. Secondly, across a wide range of broad leaf trees from various environments, it is also shown that the magnitude of estimated gradients in the activity of Rubisco within plant canopies tends to be greater for those trees with the highest Rubisco activity in their upper canopy leaves. In contrast to previous notions, it is found that in all cases the optimal within-tree gradient in photosynthetic capacity should be less than that of the vertical light profile. The model presented also calculates the leaf area index associated with these optimal gradients in photosynthetic capacity, with predictions surprisingly close to those actually observed.

As has been reported for other forest canopy types, gradients in physiologically relevant nutrients such as N and P

are more or less non-existent for Amazon forests when expressed on a dry weight basis, with lower concentrations on a leaf area basis lower down in the canopy associated with a decline in leaf mass per unit leaf area. As is also the case for δ^{13}C, and foliar carbon content, within-tree and between-tree gradients are, on average, similar.

Gradients in other physiologically relevant nutrients such as Mg and K are also reported. By contrast with the other foliar properties examined, variations in the magnitude of profiles within- and between-trees exist for Mg. Possible explanations for these observed gradients in cations as well as for the observed vertical variations in foliar carbon content and δ^{13}C are discussed.

Appendix A

Gradients of photosynthetic capacity in plant canopies

We first start with a general equation describing the light dependence of photosynthesis, this being a rectangular hyperbola, *viz*:

$$A_z = \frac{A_{\max(z)}\phi Q_z}{A_{\max(z)} + \phi Q_z} - R_z, \quad \text{(A1)}$$

where A_z represents the net CO_2 assimilation rate of a leaf at some point, z, within the canopy, $A_{\max(z)}$ is the maximum net CO_2 assimilation rate of the leaf in question (at light saturation), ϕ is the quantum yield, Q_z is the photon irradiance at the leaf surface and R_z is the rate of respiration by the leaf. Equation (A1) is of a slightly different form to that of a rectangular hyperbola usually presented (Causton and Dale, 1990), allowing a constant ϕ (independent of $A_{\max(z)}$). From both empirical and functional points of view better equations exist, for example the monomolecular (Causton and Dale, 1990) or hyperbolic minimum functions (Farquhar et al., 1980). But unfortunately, both equations lead to intransigent integrals when applied in the approach shown below (see also Buckley and Farquhar, 2004).

We first ignore respiration, allowing both $A_{\max}$ and Q to decline exponentially through the canopy according to

$$A_{\max(z)} = A_0^* e^{-k_P z};\ Q_z = Q_0 e^{-k_I z}, \quad \text{(A2)}$$

where Q_0 is the incident photon irradiance at the top of the canopy, A_0^* is the maximum (light saturated) photosynthetic rate of the leaves at the top of the canopy in the absence of respiration, k_P is an "extinction" coefficient describing the decline in photosynthetic capacity, k_I is an "extinction" coefficient describing the decline in photon irradiance, both extinction coefficients being expressed as a function of the cumulative leaf area index as measured downwards from the top of the canopy. A combination of Eq. (A1) and (A2) when integrated downwards through a canopy of leaf area index L is

$$A_C^* = \int_0^L \frac{A_0^* e^{-k_P z}\phi Q_0 e^{-k_I z}}{A_0^* e^{-k_P z} + \phi Q_0 e^{-k_I z}} dz, \quad \text{(A3)}$$

where A_C^* is the photosynthetic rate of the canopy, ignoring any respiration in the light. An analytical solution to Eq. (A3) exists, being

$$A_C^* = \frac{A_0(k_i - k_P)e^{-k_I z}\ {}_2F_1[a,b,c,\zeta]}{k_P}\Bigg|_{z=0}^{z=L}. \quad \text{(A4)}$$

Here ${}_2F_1\ [a,b,c,\zeta]$ is Gauss's hypergeometric function (Abramowitz and Stegun, 1972) with a=$k_P/(k_P-k_I)$, b=1, c= $(2k_P-k_I)/(k_I-k_P)$ and ζ=$-A_0 e^{(k_I-k_P)z}/(\phi Q_0)$. Gauss's hypergeometric function can be estimated numerically, for example using the algorithm of Forrey (1997). When k_P=k_I then Eq. (A4) is undefined, but calculation is still possible as for this special case

$$A_C^* = \frac{-A_0^*\phi Q_0 e^{-k_I z}}{k_I(A_0^* + \phi Q_0)}\Bigg|_{z=0}^{z=L} = \frac{A_0^*\phi Q_0(1 - e^{-k_I L})}{k_I(A_0^* + \phi Q_0)}. \quad \text{(A5)}$$

Note that Eq. (A5) is very similar in form to Eq. (A1) with the term $(1-e^{-k_I L})/k_I$ representing the co-ordinated decline of both light and photosynthetic capacity down the canopy.

A respiration term can be now be added to Eq. (A4) or Eq. (A5). We first take the result of Atkin et al. (2000) who showed for *Eucalyptus pauciflora* that at 30 °C the rate of respiration in the light first rapidly declines with irradiance, then subsequently increases at a much slower rate. From their data, we fitted a curve of the form

$$R_z = R_{d(z)}\left(1 - \frac{\alpha Q_z}{\beta + Q_z} + \gamma Q_z\right), \quad \text{(A6)}$$

where R_d is the (maximum) rate of foliar respiration in the dark, and with α, β and γ being fitted constants with values of 0.9575, 29.85 µmol m^{-2} s^{-1} and 5.114×10^{-5} µmol quanta µmol^{-1} CO_2, respectively (r^2=0.999). This is shown in Fig. A1a.

Numerous studies have shown that leaf respiration rates in the dark tend to scale with variations in photosynthetic capacity, this also being the case for tropical forests (Domingues et al., 2005). We can therefore express R_d as a constant fraction, f, of $A_{\max}$, a typical value of which is 0.08, although this fraction may decline to some extent with depth within the canopy (Cavaleri et al., 2008). Light response curves for a range of $A_{\max(z)}$ and with f=0.08 are shown in Fig. 1b, *viz*. Eq. A1 combined with Eq. (A6) and with $R_{d(z)}$=0.08 $A_{\max(z)}$.

Light response curves for a range of $A_{\max(z)}$ combined with Eq. A2 gives

$$R_C = \frac{f A_0 e^{-(k_P-k_I)z}\left\{Q_0\alpha k_P - (k_P+k_I)\beta e^{k_I z} + \gamma_2 Q_0 k_P\ {}_2F_1[a,b,c,\zeta]\right\}}{\beta k_P/(k_P-k_I)}\Bigg|_{z=0}^{z=L} \quad \text{(A7)}$$

with a=1, b=(k_P−k_I)/k_P, c=k_P/k_I and ζ=−$\beta e^{-k_I z}/Q_0$. As for Eq. (A4), we can also express Eq. (A6) in an alternative and simpler form for the special case of k_P=k_I *viz*

$$R_C = f A_0^* \left(\frac{(\alpha - 1)e^{-k_I z}}{k_I} - \frac{Q_0 \gamma e^{-2 k_I z}}{2 k_I} - \frac{\alpha\beta \log_e[\beta + Q_0 e^{-k_I z}]}{Q_0 k_I} \right) \Bigg|_{z=0}^{z=L}. \quad \text{(A8)}$$

In all simulations presented here, Eq. (A7) has been subtracted from Eq. (A4) (or Eq. A8 subtracted from Eq. A5) to give a net CO_2 assimilation rate, A_C=A_C^*−R_C with the hypergeometric functions solved using the algorithm of Forrey (1997). When applying this algorithm if was found, however, that as k_P→k_I sometimes the numerical solution did not converge, especially at low light where ζ could be strongly negative and a and c took on large values for the hypergeometric function in Eq. (A4). For such cases, we therefore substituted a representation of a continued equation form of the hypergeometric function which for most of the offending combinations of a, b and z did allow a stable solution to be obtained. Here we used the general approach of Lenz (1976) as modified by Thompson and Barnett (1986).

Appendix B

Evolutionarily stable versus instantaneous model solutions

From Sect. 2.3, estimates of within canopy gradients in photosynthetic capacity and leaf area index are intimately interrelated, and indeed the earliest models of canopy structure and function (Monsi and Saeki, 1953) were based on the idea that the optimal leaf area index of a canopy would be that where the lowest leaves existed at the light compensation point where daily leaf photosynthesis was just cancelled out by respiration (see also Hirose, 2005). Nevertheless, as pointed out by Anten (2002, 2005) such a calculation assumes that the optimum for an individual is not affected by the characteristics of its neighbours, being "simple optimization" in the sense of Parker and Maynard Smith (1990). That is to say, the calculations in Sect. 2.3 overlook the fact that by increasing it's L above the estimated "optimum" value, a plant may also gain in its chances of survival and increase its long term growth rate by shading its neighbour(s) within the same canopy stratum as well as its potential competitors below. Looking at Fig. 4 then, one might conclude that for any given A_0^*, the "evolutionarily stable" optimal solution with a higher L might, in fact, be somewhat to the left of the identified optimal value and with a slightly lower N_R and C_C. Alternatively, whilst still maintaining the same C_C, a tree might simply increase L through an increase in k_P, as for example in Fig. 3.

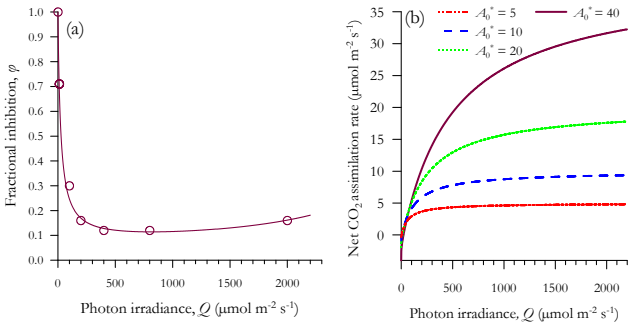

Fig. A1. Key features of the model. **(a)** Inhibition of leaf respiration in the light (Eq. A6); **(b)** Predicted variations net CO_2 assimilation rates for a range of leaf photosynthetic capacities (expressed as a maximum CO_2 assimilation rate in the absence of dark respiration, A_0^*, with units of μmol m^{-2} s^{-1}) including an allowance for inhibition of leaf respiration in the light according to Eq. (A1) with R_z from Eq. (A6) and with ϕ=0.008 mol CO_2 mol^{-1} quanta).

But what might be the magnitude of this effect? As pointed out by Anten (2002) this evolutionarily optimal L would be that where the relative losses in N_R incurred in reducing the photosynthetic gain of one's competitors was not balanced by the relative gain in increasing their losses. In a mathematical sense then, the optimal "evolutionarily stable" L would be one where

$$\frac{dN_R}{dL} \geq -\frac{dN_C}{dL}, \quad \text{(B1)}$$

with N_C representing the net carbon gain of the competitors. Computing the right-hand term is difficult for such a heterogeneous system as a tropical forest, but we have made a simple, albeit crude, attempt of the likely effect assuming the L of any tree affects the photosynthetic gain of only those trees in lower stratums within the same canopy without any direct competition between different trees sharing the same canopy layer. We assume that the affected understorey trees have a relatively low photosynthetic capacity of A_0^*=5 μmol m^{-2} s^{-1} with L=1.0 and with k_P=0.15. We emphasise that this is only a very rough estimate, designed merely to give an indication of the likely importance of the effect, also noting that it overlooks the importance of leaf production and vertical positioning as well as the dynamics of leaf production in relation to the optimisation of L (Hikosaka, 2003; Boonman et al., 2006).

Estimates of the upper tree "evolutionarily stable" L so calculated from Eq. (4) (denoted $L°$) are given in Table B1 for selected combinations of A_0^* and C_C. Also listed are estimates of L from the "individual optimization case" (Fig. 4) and a third estimate where the original Monsi and Saeki (1953) criterion is considered; *viz*. the L where the leaf at the bottom of the canopy has its photosynthetic carbon gain exactly balanced by its respiratory losses. In our case this "compensation point" represents the average photosynthesis and respiration rates over the 3.5 year period at Tapajós forest (see Sect. 2.2), and is denoted by L^*.

Table B1. Different potential "optimal" values of leaf area index and associated decay coefficients for photosynthetic capacity through the canopy, k_P (in brackets) for various combinations of total canopy photosynthetic capacity, C_C expressed in $\mu mol\,m^{-2}$ (ground area) s^{-1}, and photosynthetic capacity for leaves at the top of the canopy in the absence of dark respiration, A_0^*, expressed in $\mu mol\,m^{-2}$ (leaf area) s^{-1}. Three values are given (in order); that where the photosynthetic productivity is maximised as in Fig. 4: i.e. with no consideration of "evolutionarily stable" strategies or the need for the light compensation point, for the lowest leaves to be greater than zero; L: that where the "evolutionarily stable" leaf area index has been estimated as in Eq. (B1); L°: and that where the long term light compensation point is equal to zero (i.e. photosynthesis is exactly balanced respiration for the lowest leaves of the canopy over a 3.5 year period; L^*). NR = "Not Reached" which means this point occurred above the maximum tested leaf area index of 10.0; ND = "Not Determined", usually because the value of k_P required to fulfill these simulations was <0.0 (see text). Values in bold suggest the most likely values (see text) and lightly shaded cells correspond to the "optimal" solutions as shown in Fig. 4.

	Model	C_C=15.75	C_C=21.0	C_C=31.5	C_C=42.0	C_C=52.5	C_C=63.0
A_0^*=6	L	5.1(0.29)	4.3 (0.10)	ND	ND	ND	ND
	L°	NR	**7.2 (0.23)**	ND	ND	ND	ND
	L^*	NR	7.4 (0.24)	ND	ND	ND	ND
A_0^*=12	L	NR	8.9 (0.57)	5.4 (0.31)	4.6 (0.12)	4.2 (0.00)	ND
	L°	NR	NR	8.4 (0.36)	6.7 (0.22)	5.9 (0.10)	ND
	L^*	NR	NR	**7.9 (0.36)**	**5.5 (0.18)**	**4.5 (0.01)**	ND
A_0^*=18	L	NR	NR	9.4 (0.57)	6.2 (0.39)	5.1 (0.24)	4.7 (0.14)
	L°	NR	NR	NR	9.0 (0.42)	7.4 (0.30)	6.6 (0.22)
	L^*	NR	NR	NR	**8.0 (0.41)**	**5.5 (0.26)**	**4.5 (0.12)**

Table B1 shows that the estimated "evolutionarily stable" L° can be as much as $3\,m^2\,m^{-2}$ greater than that calculated from Fig. 4 which is not that surprising given the only very slight reductions in N_R that occur when L increases above its optimum value (Fig. 3). Note, however, that L^* is often less than L°, and for the highest A_0^*/C_C combinations, actually less than L as inferred from Fig. 4. As noted in the Sect. 6.1 this is of some consequence, because although it is conceptually possible for a leaf at the bottom of a canopy to have a net negative carbon balance and still be a net benefit to the plant (its costs to the plant in terms of being a net sink for carbohydrates being more than offset by its contribution in helping to shade a competitor), it seems this is not a physiologically viable possibility. This is because during leaf maturation, major physiological changes in phloem structure and physiology occur, meaning that it is impossible for adult leaves to act as net sinks of carbohydrates sourced from the rest of the plant (Turgeon, 2006), even if it were somehow in the plant's interest for them to do so. For trees with high A_0^*, this effect occurs at much lower L (due to relatively higher respiratory costs). This means that, despite the model as presented here initially predicting higher L with higher A_0^*, the ability for lower A_0^* trees to sustain leaves at low light levels might allow them to maintain a higher L than their faster growing counterparts (Sterck et al., 2001; Kitajima et al., 2005).

Acknowledgements. We thank our numerous South American collaborators for help with logistics and practical assistance in the field and Owen Atkin for provision of the original data shown in Fig. A1a and used for the paramaterisations of Eq. (A6). Nikos Fyllas and two anonymous referees provided useful comments on the manuscript and Shiela Wilson helped with manuscript editing.

Edited by: J. Grace

References

Abramowitz, M. and Stegun, I. A.: Hypergeometric Functions, in: Handbook of Mathematical Functions with Formulas, Graphs, and Mathematical Tables, 9th edn., New York, Dover, 555–566, 1972.

Alton, P. B. and North, P.: Interpreting shallow, vertical nitrogen profiles in tree crowns: A three-dimensional, radiative-transfer simulation accounting for diffuse sunlight, Agr. Forest Meteorol., 145, 110–124, 2007.

Anderson, J. M. and Ingram, J. S. I.: Tropical soil biology and fertility: a handbook of methods, CAB International, Wallingford, UK, 1–221, 1993.

Anten, N. P. R.: Evolutionarily stable leaf area production in plant populations, J. Theor. Biol., 217, 15–32, 2002.

Anten, N. P. R.: Optimal photosynthetic characteristics of individual plants in vegetation stands and implications for species coexistence, Ann. Botan.-London, 95, 495–506, 2005.

Ashton, P. S.: Crown characteristics of tropical trees, in: Tropical Trees as Living Systems, edited by: Tomlinson, P. B. and Zimmerman, M. H., Cambridge University Press, Cambridge, 591-615, 1978.

Atkin, O. K., Evans, J. R., Ball, M. C., Lambers, H., and Pons, T. L.: Leaf respiration of snow gum in the light and dark, interactions between temperature and irradiance, Plant Physiol., 122, 915–923, 2000.

Aragão, L. E. O. C., Shimabukaro, Y. E., Santo, F. D. B. E., and Williams, M.: Landscape pattern and spatial variability of leaf area index in Eastern Amazonia, Forest Ecol. Manag., 211, 240–256, 2005.

Basset, Y., Aberlenc, H.-P., Barrios, H., Curtelli, G., Bérenger, J.-M., Vesco, J.-P., Causse, P., Haugm, A., Hennion, A.-S., Lescobre, L., Marques, F., and O'Meara, R.: Stratification and diel activity of arthropods in a lowland rain forest in Gabon, Biol. J. Linn. Soc., 72, 585–607, 2001.

Björkman, O.: Responses to different quantum flux densities, Enc. Plant Physiol., 12, 57–107, 1981.

Boardman, N. K.: Comparative photosynthesis of sun and shade plants, Annu. Rev. Plant Physiol., 28, 355–377, 1977.

Boonman, A., Anten, N. P. R., Dueck, T. A., Jordi, W. J. R. M., van der Werf, A., Voesenek, L. A. C. J., and Pons, T. L.: Functional significance of shade-induced leaf senescence in dense canopies: An experimental test using transgenic tobacco, Am. Nat., 168, 597–607, 2006.

Boumans, P. W. J. M.: Inductively Coupled Plasma Emission Spectrometry: Part I, John Wiley & Sons, New York, 1987.

Buckley, T. N. and Farquhar, G. D.: A new analytical model for whole-leaf potential electron transport rate, Plant Cell Environ., 27, 1487–1502, 2004.

Buckley, T. N., Miller, J. D., and Farquhar, G. D.: The mathematics of linked optimisation for water and nitrogen use in a canopy, Silva Fennica, 36, 639–669, 2002.

Carswell, F. E., Meir, P., Wandelli, E. V., Bonates, I. C. M., Kruijt, B., Barbosa, E. M., Nobre, A. D., Grace, J., and Jarvis, P. G.: Photosynthetic capacity in a central Amazonian rain forest, Tree Physiol., 20, 179–186, 2000.

Causton, D. R., and Dale, M. P.: The monomolecular and rectangular hyperbola as empirical models of three *Veronica* species, Ann. Botan.-London, 65, 389–394, 1990.

Cavaleri, M., Oberbauer, S. F., and Ryan, M. G.: Foliar and ecosystem respiration in an old growth tropical forest, Plant Cell Environ., 31, 473–483, 2008.

Chang, W. H., McKean, J. W., Naranjo, J. D., and Sheather, S. J.: High-breakdown rank regression, J. Am. Stat. Assoc., 94, 205-219. 1999.

Chen, J. J., Reynolds, P., Harley, P., and Tehnunen, J.: Coordination theory of nitrogen distribution in a canopy, Oecologia, 93, 63–69, 1993.

Cromer, R. N., Kriedemann, P. E., Sands, P. J., and Stewart, L. G.: Leaf growth and photosynthetic response to nitrogen and phosphorus in seedling trees of *Gmelina arborea*, Aust. J. Plant Physiol., 20, 83–98, 1993.

DeJong, T. M. and Doyle, J. F.: Seasonal relationships between leaf nitrogen content (photosynthetic capacity) and leaf canopy light exposure in peach (*Prunus persica*), Plant Cell Environ., 8, 701–706, 1985.

De Pury, D. G. G. and Farquhar, G. D.: Simple scaling of photosynthesis from leaves to canopies without the errors of big-leaf models, Plant Cell Environ., 20, 537–557, 1997.

DIN EN ISO 11885: Determination of 33 elements by inductively coupled plasma atomic emission spectroscopy, Brussels: European Committee for Standardization, 1998.

Domingues, T. F., Berry, J. A., Martinelli, L. A., Ometto, J. P. H. B., and Ehleringer, J. R.: Parameterization of canopy structure and leaf-level gas exchange for an Amazonian tropical rain forest (Tapajós National Forest, Pará, Brazil), Earth Interactions, 9, Paper No. 17, 2005.

Domingues, T. F., Meir, P., Saiz, G., Feldpausch, T. R., Veenendaal, E. M., Schrodt, F., Bird, M., Djagbletey, G., Hien, F., Compaore, H., Diallo, A., Grace, J., and Lloyd, J.: Co-limitation of photosynthetic capacity by nitrogen and phosphorus in West Africa woodlands, Plant Cell Environ., 33, 959–980, 2010.

Dominy, N. J., Lucas, P. W., and Wright, S. J.: Mechanics and chemistry of rain forest leaves; canopy and understory compared, J. Exp. Bot., 54, 2007–2014, 2003.

Downum, K., Lee, D., Hallé, F., Quirke, M., and Towers, N.: Plant secondary compounds in the canopy and understory of a tropical rain forest in Gabon, J. Trop. Ecol., 17, 477–481, 2001.

Duursma, R. A. and Marshall, J. D.: Vertical canopy gradients in δ^{13}C correspond with leaf nitrogen content in a mixed-species conifer forest, Trees, 20, 496-506, 2006.

Ellsworth, D. S. and Reich, P. B.:Canopy structure and vertical patterns of photosynthesis and related leaf traits in a deciduous forest, Oecologia, 96, 169–178, 1993.

Evans, J. R.: Photosynthesis and nitrogen relationships in leaves of C_3 plants, Oecologia, 78, 9–19, 1989.

Evans, J. R. and Poorter, H.: Photosynthetic acclimation of plants to growth irradiance: the relative importance of specific leaf area and nitrogen partitioning in maximizing carbon gain, Plant Cell Environ., 24, 755–767, 2001.

Farquhar, G. D., von Caemmerer, S., and Berry, J. A.: A biochemical model of photosynthetic CO_2 assimilation in leaves of C_3 species, Planta, 149, 78–90, 1980.

Farquhar, G. D.: Models of integrated photosynthesis of cells and leaves, Philos. T. Roy. Soc. Lon. B, 323, 357–367, 1989.

Field, C. B.: Allocating leaf nitrogen for the maximization carbon gain: leaf age as a control on the allocation program, Oecologia, 56, 314–347, 1983.

Field, C. B. and Mooney, H. A.: The photosynthesis-nitrogen relationship in wild plants, in: The Economy of Plant Form and Function, edited by: Givnish, T. J., Cambridge University Press, Cambridge, 25–55, 1986.

Forrey, R. C.: Computing the hypergeometric function, J. Comp. Phys., 137, 79–100, 1997.

Fyllas, N. M., Patiño, S., Baker, T. R., Bielefeld Nardoto, G., Martinelli, L. A., Quesada, C. A., Paiva, R., Schwarz, M., Horna, V., Mercado, L. M., Santos, A., Arroyo, L., Jiménez, E. M., Luizão, F. J., Neill, D. A., Silva, N., Prieto, A., Rudas, A., Silviera, M., Vieira, I. C. G., Lopez-Gonzalez, G., Malhi, Y., Phillips, O. L., and Lloyd, J.: Basin-wide variations in foliar properties of Amazonian forest: phylogeny, soils and climate, Biogeosciences, 6, 2677–2708, doi:10.5194/bg-6-2677-2009, 2009.

Gardemann, A., Schimikat, A., and Heldt, H. W.: Control of CO_2 fixation: Regulation of stromal fructose-1,6-bisphosphate in spinach by pH and Mg^{2+} concentration, Planta, 168, 536–545, 1986.

Gleason, S. M. and Ares, A.: Photosynthesis, carbohydrate storage and survival of a native and an introduced tree species in relation to light and defoliation, Tree Physiol., 24, 1087–1097, 2004.

Goulden, M. L., Miller, S. D., da Rocha, H. R., Menton, M. C., de Freitas, H. C., Figueira, A. M. E. S., and de Sousa, C. A. D.: Diel and seasonal patterns of tropical forest CO_2 exchange, Ecol. Appl., 14(4), S42–S54, 2004.

Grubb, P. J. and Edwards, P. J.: Studies of mineral cycling in a montane rain forest in New Guinea III, The distribution of mineral elements in the above-ground material, J. Ecol., 72, 623–648, 1982.

Hallé, F., Oldeman, R. A. A., and Tomilson, P. B.: Tropical Trees and Forests, An Architectural Analysis, Springer-Verlag, Berlin, 1978.

Haxeltine, A. and Prentice, I. C.: A general model for the light-use efficiency of primary production, Funct. Ecol., 10, 551–561, 1996.

Hikosaka, K.: A Model of dynamics of leaves and nitrogen in a plant canopy: An integration of canopy photosynthesis, leaf life span, and nitrogen use efficiency, Am. Nat., 162, 149–164, 2003.

Hikosaka, K.: Leaf canopy as a dynamic system: ecophysiology and optimality in leaf turnover, Ann. Botan.-London, 95, 521, 2005.

Hirose, T.: Development of the Monsi-Saeki theory on canopy structure and function, Ann. Botan.-London, 95, 483, 2005.

Hirose, T. and Werger, M. J. A.: Maximizing daily canopy photosynthesis with respect to the leaf nitrogen allocation pattern in the canopy, Oecologia, 72, 520–526, 1987.

Hollinger, D. Y.: Optimality and nitrogen allocation in a tree canopy, Tree Physiol., 16, 627–634, 1996.

Hurry, V., Igamberdiev, A. U., Keerberg, O., Pärnik, T., Atkin, O. K., Zaragoza-Castells, J., and Gardeström, P.: Respiration in photosynthetic cells: gas exchange components, interactions with photorespiration and the operation of mitochondria in the light, in: Plant Respiration: From Cell to Ecosystem. Advances in Photosynthesis and Respiration, vol 18, edited by: Lambers, H. and Ribas-Carbós, M., Springer, Dordrecht, The Netherlands, 43–61, 2005.

Hutyra, L. R., Munger, J. W., Gottlieb, E. W., Daube, B. C., Camargo, P. B., and Wofsy, S. C.: Seasonal controls on the exchange of carbon and water in an Amazonian rain forest, J. Geophys. Res., 112, G03008, doi:10.1029/2006JG000365, 2007.

Jarvis P. G., James, B. G., and Landsberg, J. J.: Coniferous forest, in: Vegetation and Atmosphere, edited by: Monteith, J. L., Academic Press, London, 171–204, 1976.

Kato, M., Inoue, T., Hamid, A. A., Nagamitsu, T., Merdek, M. B., Nona, A. R., Itino, T., Yamane, S., and Yumoto, T.: Seasonality and vertical structure of light-attracted insect communities in a Dipterocarp forest in Sarawak, Res. Popul. Ecol., 37, 59–79, 1995.

Kellner, J. R., Clark, J. B., and Hubbell, S. P.: Pervasive canopy dynamics produce short term stability in a tropical forest landscape, Ecol. Lett., 12, 155–164, 2009.

Kenzo, T., Ichie, T., Watanabe, Y., Yoneda, R., Nonomiya, I., and Koike, T.: Changes in photosynthesis and leaf characteristics with tree height in five diperocarp species in a tropical rain forest, Tree Physiol., 26, 865–873, 2006.

Kitajima, K., Mulkey, S. S., and Wright, S. J.: Variation in crown light utilization characteristics among tropical canopy trees, Ann. Botan.-London, 95, 535–547, 2005.

Koike, F., Riswan, S., Partomihardjo, T., Suzuki, E., and Hotta, M.: Canopy structure and insect community distribution in a tropical rain forest of West Kalimantan, Selbyana, 19, 147–154, 1998.

Kull, O. and Niinemets, U.: Distribution of photosynthetic properties in leaf canopies; comparison of species with different shade tolerance, Funct. Ecol., 12, 472–479, 1998.

Lebaudy, A., Vavasseur, A., Hosy, E., Dreyer, D., Leonhardt, N., Thibaud, J. B., Véry, A.-A., Simonneau, T. and Hervé, S.: Plant adaptation to fluctuating environment and biomass production are strongly dependent on guard cell potassium channels, P. Natl. Acad. Sci. USA, 105, 5271–5276, 2008.

Leigh, R. A. and Wyn Jones, R. G.: A hypothesis relating critical potassium concentrations for growth to the distribution and function of this ion in the plant cell, New Phytol., 97, 1–13, 1984.

Lentz, W. J.: Generating Bessel functions in Mie scattering calculations using continued fractions, Appl. Optics, 15, 668–671, doi:10.1364/AO.15.000668, 1976.

Lichtenthaler, H. K., Buschmann, C., Doll, M., Fietz, H.-J., Bach, T., Kozel, U., Meier, D., and Rahmsdorf, U.: Photosynthetic activity, chloroplast ultrastructure, and leaf characteristics of high-light and low-light plants and of sun and shade leaves, Photosynth. Res., 2, 115–141, 1981.

Lloyd, J., Grace, J., Miranda, A. C., Meir, P., Wong, S.-C., Miranda, H. S., Wright, I. R., Gash, J. H. C., and MacIntyre, J. A.: A simple calibrated model of Amazon rain forest productivity based of leaf biochemical properties, Plant Cell Environ., 18, 1129–1145, 1995.

Lloyd, J., Kruijt, B., Hollinger, D. Y., Grace, J., Francey, R. J., Wong, S.-C., Kelliher, F. M., Miranda, A. C., Farquhar, G. D., Gash, J. H. C., Vygodskaya, N. N., Wright, I. R., Miranda, H. S., and Schulze, E.-D.: Vegetation effects on the isotopic composition of atmospheric CO_2 as local and regional scales: Theoretical aspects and a comparison between rainforest in Amazonia and a boreal forest in Siberia, Aust. J. Plant Physiol., 23, 371–399, 1996.

Lloyd, J., Bird, M. I., Veenendaal, E. M., and Kruijt, B.: Should phosphorus availability be constraining moist tropical forest responses to increasing CO_2 concentrations? in: Global Biogeochemical Cycles in the Climate System, edited by: Schulze, E., Heimann, M., Harrison, S., Holland, E., Lloyd, J., Prentice, I. C., and Schimel, D., Academic Press, San Diego, CA, 95–114, 2001.

Lovelock, C. E., Kyllo, D., Popp, M., Isopp, H., Virgo, A., and Winter, K.: Symbiotic vesicular-arbuscular mycorrhizae influence maximum rates of photosynthesis in tropical tree seedlings grown under elevated CO_2, Austral. J. Plant Physiol., 24, 185–194, 1997.

Lowman, M. D.: Leaf growth dynamics and herbivory in five species of Australian rain-forest canopy trees, J. Ecol., 80, 433–447, 1992.

Lowman, M. D. and Box, J. D.: Variation in leaf toughness and phenolic content among five species of Australian rain forest trees, Aust. J. Ecol., 8, 17–25, 1983.

Lynch, J. P. and Ho, M. D.: Rhizoeconomics: carbon costs of phosphorus acquisition, Plant Soil, 269, 45–56, 2005.

Malavolta, E., Vitti, G. C., and de Oliveira, S. A.: Avaliação do estado nutricional das plantas: principios e aplicações. Associação Brasileira para Pesquisa da Potassa e do Fosfato, 1989.

Masle, J., Farquhar, G. D., Gifford, R. M.: Growth and carbon economy of wheat seedlings as affected by soil resistance to penetration and ambient partial pressure of CO_2, Aust. J. Plant Physiol., 17, 465-487, 1990.

McGill, B. J., Enquist, B. J., Weiherc, E., and Westoby, M.: Rebuilding community ecology from functional traits, Trends Ecol. Evol., 21, 178–185, 2006.

Meinzer, F. C., Campanello, P. I., Domec, J.-C., Gatti, M. G., Goldstein, G., Villalobs-Vega, and Woodruff, D. R.: Constraints on physiological function associated with branch architecture and wood density in tropical forest trees, Tree Physiol., 28., 1609–1617, 2008.

Meir, P., Kruijt, B., Broadmeadow, M., Barbosa, E., Kull, O., Carswell, F., Nobre, A., and Jarvis, P. G.: Acclimation of photosynthetic capacity to irradiance in tree canopies in relation to leaf nitrogen and leaf mass per unit area, Plant Cell Environ., 25, 343–357, 2002.

Mercado, L. M., Lloyd, J., Carswell, F., Malhi, Y., Meir, P., and Nobre, A. D.: Modelling Amazonian forest eddy covariance data: a comparison of big leaf versus sun/shade models for the C-14 tower at Manaus I. Canopy photosynthesis, Acta Amazonica, 36, 69–82, doi:10.1590/S0044-59672006000100009, 2006.

Mercado, L. M., Huntingford, C., Gash, J. H. C., Cox, P. M., and Jogireddy, V. A.: Improving the representation of radiation interception and photosynthesis for climate model applications, Tellus B, 59, 553–565, 2007.

Mercado, L. M., Lloyd, J., Dolman, A. J., Sitch, S., and Patiño, S.: Modelling basin-wide variations in Amazon forest productivity - Part 1: Model calibration, evaluation and upscaling functions for canopy photosynthesis, Biogeosciences, 6, 1247–1272, doi:10.5194/bg-6-1247-2009, 2009.

Miyazawa, S.-I., Suzuki, A. A., Sone, K., and Terashima, I.: Relationships between light, leaf nitrogen and nitrogen remobilisation in the crowns of mature evergreen *Quercus glauca* trees, Tree Physiol., 24, 1157–1164, 2004.

Monsi, M. and Saeki, T.: Über den Lichtfaktorin den Pflanzengesellschaften und seine Bedeutung fur den Stoffproduction, Jap. J. Bot., 14, 14–52, 1953.

Myers, B. J., Robichaux, R. H., Unwin, G. L., and Craig, I. E.: Leaf water relations and anatomy of a tropical rainforest tree species vary with crown position, Oecologia, 74, 81–85, 1987.

Niinemets, U.: Photosynthesis and resource distribution through plant canopies, Plant Cell Environ., 30, 1052–1071, 2007.

Niinemets, U., Söber, A., Kull, O., Hartung, W., and Tenhunen, J. D.: Apparent controls on leaf conductance by soil water availability and via light-acclimation of foliage structural and physiological properties in a mixed deciduous temperate forest, Int. J. Plant Sci., 160, 707–721, 1999.

Niinemets, U. and Valladares, F.: Photosynthetic acclimation to simultaneous and interacting environmental stresses along natural light gradients: Optimality and constraints, Plant Biol., 6, 254–268, 2004.

Niinemets, U., Sonninen, E., and Tobias, M.: Canopy gradients in leaf intercellular CO_2 mole fractions revisited: interactions between leaf irradiance and water stress need consideration, Plant Cell Environ., 27, 569–583, 2004.

Oberbauer, S. F., Strain, B. R., and Riechers, G. H.: Field water relations of a wet-tropical forest tree species, *Pentaclethra macroloba* (Mimosaceae), Oecologia, 71, 369–374, 1987.

Olsen, S. R. and Sommers, E. L.: Phosphorus Soluble in Sodium Bicarbonate, Methods of Soil Analysis, Part 2, Chemical and Microbiological Properties, edited by: Page, A. L., Miller, P. H., and Keeney D. R., American Society of Agronomy, Soil Science Society of America, Madison, WIS, 404–430, 1982.

Ometto, J. P. H. B., Ehleringer, J. R., Domingues, T. F., Ishida, F. Y., Berry, J., Higuchi, N., Flanagan, L., Nardoto, G. B., and Martinelli, L. A..: The stable carbon and nitrogen isotopic composition of vegetation of the Amazon region, Brazil, Biogeochemistry, 79, 251–274, 2006.

Parker, G. and Maynard Smith, J.: Optimization theory in evolutionary biology, Nature, 348, 27–33, 1990.

Patiño, S., Lloyd, J., Paiva, R., Baker, T. R., Quesada, C. A., Mercado, L. M., Schmerler, J., Schwarz, M., Santos, A. J. B., Aguilar, A., Czimczik, C. I., Gallo, J., Horna, V., Hoyos, E. J., Jimenez, E. M., Palomino, W., Peacock, J., Peña-Cruz, A., Sarmiento, C., Sota, A., Turriago, J. D., Villanueva, B., Vitzthum, P., Alvarez, E., Arroyo, L., Baraloto, C., Bonal, D., Chave, J., Costa, A. C. L., Herrera, R., Higuchi, N., Killeen, T., Leal, E., Luizão, F., Meir, P., Monteagudo, A., Neil, D., Núñez-Vargas, P., Peñuela, M. C., Pitman, N., Priante Filho, N., Prieto, A., Panfil, S. N., Rudas, A., Salomão, R., Silva, N., Silveira, M., Soares deAlmeida, S., Torres-Lezama, A., Vásquez-Martínez, R., Vieira, I., Malhi, Y., and Phillips, O. L.: Branch xylem density variations across the Amazon Basin, Biogeosciences, 6, 545–568, doi:10.5194/bg-6-545-2009, 2009.

Pons, T. L., Schieving, F., Hirose, T., and Werger, M. J. A.: Optimization of leaf nitrogen allocation for canopy photosynthesis in Lysimachia vulgaris, in: Causes and consequences of variation in growth rate and productivity of higher plants, edited by: Lambers, H., Cambridge, M. L., Konings, H., and Pons, T. L., SPB Publishing, The Hague, The Netherlands, 175–186, 1990.

Poorter, H., Niinemets, U., Poorter, L., Wright, I. J., and Villar, R.: Causes and consequences of variation in leaf mass per area (LMA): a meta-analysis, New Phytol., 182, 565-588, 2009.

Poorter, L., Kwant, R., Hernandez, R., Medina, E., and Werger, M. J. A.: Leaf optical properties in Venezuelan cloud forest trees, Tree Physiol., 20, 519–526, 2000.

Poorter, L., Bongers, F., Sterck, F. J., and Wöll, H.: Architecture of 53 rain forest tree species differing in adult stature and shade tolerance, Ecology, 84, 602–612, 2003.

Poorter, L., Bongers, L., and Bongers, F.: Architecture of 54 moist-forest tree species: traits, trade-offs, and functional groups, Ecology, 87, 1289–1301, 2006.

Popma, J., Bongers, F., and Werger, M. J. A.: Gap-dependence and leaf characteristics of trees in a tropical rain forest in Mexico, Oikos, 63, 207–214, 1992.

Portis, A. R.: Regulation of ribulose-1,5-bisphosphate carboxylase/oxygenase activity, Ann. Rev. Plant Phys., 43, 415–437, 1992.

Poseda, J. M., Lechowicz, M. J., and Kitajima, K.: Optimal photosynthetic use of light by tropical tree crowns achieved by adjustment of individual leaf angles and nitrogen content, Ann. Bot., 103, 795–805, 2009.

Pottosin, I. I. and Schönkmecht, G.: Ion channel permeable for divalent and monovalent cations in native spinach thylakoid membranes, J. Membrane Biol., 152, 223–233, 1996.

Prior, L. D., Bowman, D. M. J. S., and Eamus, D.: Seasonal differences in leaf attributes in Australian tropical tree species: family and habitat comparisons, Funct. Ecol., 18, 707-718, 2004.

Quesada, C. A., Lloyd, J., Schwarz, M., Patiño, S., Baker, T. R., Czimczik, C., Fyllas, N. M., Martinelli, L., Nardoto, G. B., Schmerler, J., Santos, A. J. B., Hodnett, M. G., Herrera, R., Luizão, F. J., Arneth, A., Lloyd, G., Dezzeo, N., Hilke, I., Kuhlmann, I., Raessler, M., Brand, W. A., Geilmann, H., Moraes Filho, J. O., Carvalho, F. P., Araujo Filho, R. N., Chaves, J. E., Cruz Junior, O. F., Pimentel, T. P., and Paiva, R.: Variations in chemical and physical properties of Amazon forest soils in relation to their genesis, Biogeosciences, 7, 1515–1541, doi:10.5194/bg-7-1515-2010, 2010.

Raaimakers, D., Boot, R. G. A., Dijkstra, R., Pot, S., and Pons, T.: Photosynthetic rates in relation to leaf phosphorus content in pioneer climax tropical rain forest trees, Oecologia, 102, 120–125, 1995.

Rabash, J., Steele, F., Browne, W., and Prosser, B.: A User's Guide to MLWiN Version 2.0, Centre for Multilevel Modelling, Institute of Education, University of London, London, UK, 2004.

Rajendrudu, G. and Naidu, C. V.: Leaf gas exchange capacity in relation to leaf position on the stem of field grown teak (*Tectona grandis*), Photosynthetica, 34, 45–55, 1997.

Reich, P., Ellsworth, D. S., and Uhl, C.: Leaf carbon and nutrient assimilation and conservation in species of differing successional status in an oligotrophic Amazonian forest, Funct. Ecol., 9, 65–76, 1995.

Reich, P. B., Walters, M. B., Ellsworth, D. S., Vose, J. M., Volin, J. C., Gresham, C., and Bowman, W. D.: Relationships of leaf dark respiration to leaf nitrogen, specific leaf area and leaf life-span: a test across biomes and functional groups, Oecologia, 114, 471–482, 1998.

Reich, P. B., Wright, I. J., Cavender-Bares, J., Craine, J. M., Oleksyn, J., Westoby, M., and Walters, M. B.: The Evolution of Plant Functional Variation: Traits, Spectra, and Strategies, Int. J. Plant Sci., 164(S3), S143-S164, 2003.

Rijkers, T., Pons, T. L., and Bongers, F.: The effect of tree height and light availability on photosynthetic leaf traits of four neotropical species differing in shade tolerance, Funct. Ecol., 14, 77–86, 2000.

Rozendaal, D. M. A., Hurdato, V. H., and Poorter, L.: Plasticity in leaf traits of 38 tropical tree species in response to light: relationships with light demand and adult stature, Func. Ecol., 20, 207–216, 2006.

Sands, P. J.: Modelling canopy production, II. From single-leaf photosynthetic parameters to daily canopy photosynthesis, Aust. J. Plant Physiol., 22, 603–614, 1995.

Santiago, L. S., Goldstein, G., Meinzer, F. C., Fisher, J. B., Machado, K., Woodruff, D., and Jones, T.: Leaf photosynthetic traits scale with hydraulic conductivity and wood density in Panamanian forest canopy trees, Oecologia, 140, 543–550, 2004.

Sellers, P. J., Collatz, G. J., Randall, D. A., Dazlich, D. A., Zhang, C., Berry, J. A., Field, C. B., Collelo, G. D., and Bounoua, L.: A Revised Land Surface Parameterization (SiB2) for Atmospheric GCMS, Part I: Model Formulation, J. Climate, 9, 676–705, 1996.

Shaul, O.: Magnesium function and transport in plants; the tip of the iceberg, Biometals, 15, 309–323, 2002.

Shuttleworth, W. J.: Micrometeorology of temperate and tropical forest, Philos. T. Roy. Soc. Lond. B, 324, 299–334, 1989.

Sitch, S., Smith, B., Prentice, I. C., Arneth, A., and Bondeau, A.: Evaluation of ecosystem dynamics, plant geography and terrestrial carbon cycling in the LPJ dynamic global vegetation model, Global Change Biol., 9, 161–185, 2003.

Snijders, T. A. B. and Bosker, R. J.: Multilevel analysis, Sage Publications, London, UK, 1999.

Specht, A. and Turner, J.: Foliar nutrient concentrations in mixed-species plantations of subtropical cabinet timber species and their potential as a management tool, Forest Ecol. Manag., 233, 324-337, 2006

Sterck, F. J., Rijkers, T., and Bongers, F.: Effects of tree height and light availability on plant traits at different organisational levels, Monographiae Biologicae, 289–300, 2001.

Sterck, F. J., van Gelder, A., and Poorter, L.: Mechanical branch constraints contribute to life-history variation across tree species in a Bolivian forest, J. Ecol., 94, 1192–1200, 2006.

Stockhoff, B. A.: Maximization of daily canopy photosynthesis: effects of herbivory on optimal nitrogen distribution, J. Theor. Biol., 169, 209–220, 1994.

Sutton, S. L.: The spatial distribution of flying insects, in: Tropical Rain Forest Ecosystems.,Bigeographical and Ecological Studies, edited by: Lieth, H. and Werger, M. J. A., Elsevier, Amsterdam, 427–436, 1989.

Syvertsen, J. P., Lloyd, J., McConchie, C., Kriedemann, P. E., and Farquhar, G. D.: On the site of biophysical constraints to CO_2 diffusion through the mesophyll of thick hyperstomatous leaves, Plant Cell Environ. 18, 149–157, 1995.

Terashima, I., Araya, T., Miyazawa, S. I., Sone, K., and Yano, S.: Construction and maintenance of the optimal photosynthetic systems of the leaf, herbaceous plant and tree: an eco-developmental treatise, Ann. Botan.-London, 95, 507, 2005.

Terpstra, J. T. and McKean, J. W.: Rank-Based Analyses of Linear Models Using R, J. Statist. Softw., 14, 7, 2005.

Thomas, S. C. and Bazzaz, F. A.: Asymptotic tree height as a predictor of photosynthetic characteristics in Malaysian rain forest trees, Ecology, 80, 1607–1622, 1999.

Thompson, I. J. and Barnett, A. R.: Coulomb and Bessel functions of complex arguments and order, J. Comput. Phys., 490–509, 1986.

Tong, P. S. and Ng, F. S. P.: Effect of light intensity on growth, leaf production, leaf lifespan and leaf nutrient budgets of *Acacia magnium*, *Cinnamomum inders*, *Dyera costulata*, *Eusideroxylon zwageri* and *Shorea Roxburghii*, J. Trop. For. Sci., 20, 218–234, 2008.

Townsend, A. R., Asner, G. P., and Cleveland, C. C.: The biogeochemical heterogeneity of tropical forests, Trends Ecol. Evol., 23, 424–431, 2008.

Turgeon, R.: Phloem loading: how leaves gain their independence, Bioscience, 56, 15–24, 2006.

Turner, I. M.: The Ecology of Trees in the Tropical Forest, Cambridge University Press, Cambridge, UK, 2001.

Vitousek, P. M.: Litterfall, nutrient cycling and nutrient limitation in tropical forest, Ecology, 65, 285–298, 1984.

Warren, C. R., Adams, M. A., and Chen, Z. L.: Is photosynthesis related to concentrations of nitrogen and Rubisco in leaves of Australian native plants?, Aust. J. Plant Physiol., 27, 407–416. 2000.

Werner, R. A. and Brand, W. A.: Referencing strategies and techniques in stable isotope ratio analysis, Rapid Commun. Mass Sp., 15, 501–519, 2001.

Werner, R. A., Bruch, B. A., and Brand, W. A.: ConFlo III – An interface for high precision δ^{13}C and δ^{15}N analysis with an extended dynamic range, Rapid Commun. Mass Sp., 13, 1237–1241, 1999.

Wirth, R., Weber, B., and Ryel, R. J.: Spatial and temporal variability of canopy structure in a tropical moist forest, Acta Oecol., 22, 235–244, 2001.

Woodward, F. I. and Lomas, M. R.: Vegetation dynamics – simulating responses to climatic change, Biol. Rev., 79, 643–670, doi:10.1017/S1464793103006419, 2004.

Wright, I. J., Reich, P. B., Westoby, M., Ackerly, D. D., Baruch, Z., Bongers, F., Cavender-Bares, J., Chapin, T., Cornelissen, J. H., Diemer, M., Flexas, J., Garnier, E., Groom, P. K., Gulias, J., Hikosaka, K., Lamont, B. B., Lee, T., Lee, W., Lusk, C., Midgley, J. J., Navas, M. L., Niinemets, U., Oleksyn, J., Osada, N., Poorter, H., Poot, P., Prior, L., Pyankov, V. I., Roumet, C., Thomas, S. C., Tjoelker, M. G., Veneklaas, E. J., and Villar, R.: The worldwide leaf economics spectrum, Nature, 428, 821–827, 2004.

Wright, I. J., Leishman, M. R., Read, C., and Westoby, M.: Gradients of light availability and leaf traits with leaf age and canopy position in 28 Australian shrubs and trees, Funct. Plant Biol., 43, 407–419, 2006.